mAbs 6:1, 219–235; January/February 2014; © 2014 Landes Bioscience

Antibody light chain variable domains and their biophysically improved versions for human immunotherapy

Dae Young Kim[1], Rebecca To[1], Hiba Kandalaft[1], Wen Ding[1], Henk van Faassen[1], Yan Luo[1,†], Joseph D Schrag[2], Nadereh St-Amant[3,‡], Mary Hefford[3], Tomoko Hirama[1,§], John F Kelly[1], Roger MacKenzie[1,4], and Jamshid Tanha[1,4,5,*]

[1]Human Health Therapeutics; National Research Council Canada; Ottawa, ON Canada; [2]Human Health Therapeutics; National Research Council Canada; Montréal, QC Canada; [3]Centre for Vaccine Evaluation; Biologics and Genetic Therapies Directorate; Health Canada; Ottawa, ON Canada; [4]School of Environmental Sciences; Ontario Agricultural College; University of Guelph; Guelph, ON Canada; [5]Department of Biochemistry, Microbiology, and Immunology; University of Ottawa; Ottawa, ON Canada

Current affiliation: [†]Caprotec Bioanalytics GmbH; Berlin, Germany; [‡]Canadian Nuclear Safety Commission; Ottawa, ON Canada; [§]5-2301 Kotesashicho 1-chome; Tokorozawa, Japan

Keywords: V_L, single-domain antibody, disulfide linkage, thermal stability, protease resistance

Abbreviations: CDR, complementarity-determining region; CID, collision induced dissociation; DDA, data dependent analysis; ETD, electron transfer dissociation; Fab, fragment antigen-binding; FR, framework region; HBS-EP buffer, 10 mM HEPES, pH 7.4, 150 mM NaCl, 3 mM EDTA and 0.005% P20 surfactant; GI, gastrointestinal; K_D, equilibrium dissociation constant; MALS, multiangle light scattering; Mapp, apparent molecular mass; M_{for}, formula molecular mass; M_{MALS}, molecular mass determined by MALS; MS, mass spectrometry; RU, resonance unit; sdAb, single-domain antibody; SEC, size-exclusion chromatography; scFv, single chain Fv fragment of an antibody; SPR, surface plasmon resonance; T_m, melting temperature; TRE, thermal refolding efficiency; V_H, antibody heavy chain variable domain; V_{HH}, camelid heavy chain antibody variable domain; V_L, antibody light chain variable domain; VNAR, shark IgNAR (Ig New Antigen Receptor) variable domain

We set out to gain deeper insight into the potential of antibody light chain variable domains (V_Ls) as immunotherapeutics. To this end, we generated a naïve human V_L phage display library and, by using a method previously shown to select for non-aggregating antibody heavy chain variable domains (VHs), we isolated a diversity of V_L domains by panning the library against B cell super-antigen protein L. Eight domains representing different germline origins were shown to be non-aggregating at concentrations as high as 450 μM, indicating VL repertoires are a rich source of non-aggregating domains. In addition, the V_Ls demonstrated high expression yields in *E. coli,* protein L binding and high reversibility of thermal unfolding. A side-by-side comparison with a set of non-aggregating human V_Hs revealed that the V_Ls had similar overall profiles with respect to melting temperature (T_m), reversibility of thermal unfolding and resistance to gastrointestinal proteases. Successful engineering of a non-canonical disulfide linkage in the core of V_Ls did not compromise the non-aggregation state or protein L binding properties. Furthermore, the introduced disulfide bond significantly increased their T_ms, by 5.5–17.5 °C, and pepsin resistance, although it somewhat reduced expression yields and subtly changed the structure of V_Ls. Human V_Ls and engineered versions may make suitable therapeutics due to their desirable biophysical features. The disulfide linkage-engineered V_Ls may be the preferred therapeutic format because of their higher stability, especially for oral therapy applications that necessitate high resistance to the stomach's acidic pH and pepsin.

Introduction

As antibody-based therapeutics, full-length monoclonal antibodies have little competition so far.[1-3] In fact, most approved monoclonal antibodies and those in regulatory review are canonical IgG antibodies (www.landesbioscience.com/journals/mabs/about/). The disadvantages of these molecules, such as costly and time-consuming production in mammalian cell lines, large (~150 kDa) and complex molecular structures, poor tissue penetration and inability to access cryptic epitopes, and the fact that the Fc portion of the antibody is not needed in many instances or may even be harmful, have resulted in the creation of a niche that can be occupied by antibody fragments.[2,4,5] These smaller antibody fragments, including single-domain antibodies (sdAbs), have unique features that may make them the preferred therapeutic format for many applications. Currently, there are

*Correspondence to: Jamshid Tanha; E-mail: jamshid.tanha@nrc-cnrc.gc.ca
Submitted: 09/11/2013; Revised: 10/15/2013; Accepted: 10/16/2013
http://dx.doi.org/10.4161/mabs.26844

numerous antibody fragments in clinical development, with some being sdAbs.[2,4]

sdAbs, e.g., human V_Hs, human V_Ls, camelid V_HHs, have become a viable option in the antibody-based therapeutic tool box that also includes IgGs, antigen-binding fragments (Fabs), single chain Fv fragments (scFvs), and their many derivatives. Appealing features of sdAbs include their high affinity (nM - pM equilibrium dissociation constant (K_D) range) for cognate antigens,[6-29] small size (~15 kDa) and simple structure, single domain nature, modularity, low immunogenicity, high-level expression in microorganisms such as bacteria, high thermal, chemical and protease stabilities, high solubility and aggregation resistance, ability to access cryptic epitopes, and ease of genetic manipulation and display library construction.[5,30,31] V_HHs are more convenient to obtain due to their better biophysical properties and the existence and accessibility of in vivo naïve and immune V_HH repertoire sources, but human V_Hs and V_Ls have the perceived advantage of being less immunogenic in human therapy. A number of reports have implied human V_Ls may be superior therapeutic candidates compared with human V_Hs because of their lower tendency to aggregate,[32-34] which may translate to lower immunogenicity and in turn higher therapeutic efficacy for V_Ls.

In vivo, human V_L constructs are the result of genetic recombination between germline gene segments V_L and J_L. The first two complementarity-determining regions (CDR1 and CDR2) and a part of the CDR3 up to residue 95 are encoded by V_L segment genes; the rest of the CDR3 and the entire framework region (FR) 4 are encoded by J_L gene segments.[35] Human V_Ls are classified as either κ or λ subtypes, with seven $V_κ$ gene segment subgroups ($V_κ$1–7) within the κ class and 11 $V_λ$ gene segment subgroups ($V_λ$1–11) within the λ class (http://www.imgt.org/).[36,37] In general, $V_κ$ domains exhibit higher solubility and stability than $V_λ$ domains, possibly due to a higher packing density in their upper core and a more hydrophilic C-terminus, and among the $V_κ$ subgroups, $V_κ$3 subgroup members exhibit the best properties in terms of solubility and thermodynamic stability.[33,38] A significant proportion of human V_Ls, predominantly of $V_κ$ class, bind to the B cell super-antigen protein L.[39-41]

V_L domains are similar to V_Hs in terms of overall structure. They are composed of two β-sheets that are formed by several anti-parallel β-strands and pack face-to-face to form β-sandwich structures.[42] Also, similar to V_Hs, they possess a pair of cysteine residues at spatially equivalent positions (Kabat positions 23 and 88)[43] that form a highly conserved disulfide linkage. This linkage, which pins together the two β-sheets in the core of V_L domains, plays a critical role in maintaining the structural integrity of V_Ls.[44,45] Previously, it was shown that engineering an additional disulfide linkage in the core of a set of human V_Hs improved their aggregation resistance and thermostability.[46,47] Given the overall structural similarity between V_H and V_Ls, it is hypothesized that the same engineering approach, with similar stability improvements, should be applicable to V_Ls.

Here, to further explore the merits of human V_Ls as therapeutic modalities, we set out to perform an extensive biophysical characterization of a set of test V_Ls. We constructed a naïve human V_L phage display library, and from it isolated a diversity of domains with protein L binding property by a phage selection method that was previously shown to be highly selective for non-aggregating human V_H domains.[48] We then characterized a representative sample of V_Ls for properties such as expression yield, non-aggregation, thermal stability, reversible thermal unfolding, structural integrity, and protease resistance. Next, we determined if a non-canonical disulfide linkage engineering approach previously shown to improve the thermostability and protease resistance of camelid V_HHs and human V_Hs[46,47,49-52] would do the same for the present V_Ls. Thus, we engineered human V_Ls with an additional, non-canonical disulfide linkage between Cys48 and Cys64 in β-strands C' and D. We then performed pair-wise biophysical comparisons between wild-type and their corresponding Cys mutant domains.

Results

Identification and sequence analysis of human V_Ls

Essentially the same selection method employed to isolate non-aggregating V_Hs from a human V_H phage display library was applied to a human V_L library for isolating soluble, monomeric V_Ls.[48] A human V_L library with a size of 3×10^6 transformants was constructed. Twenty-four clones (plaques) from the library titer plates were isolated and their V_L genes were amplified by PCR and then sequenced. The sequences were diverse in terms of germ-line origin, although 75% of the V_Ls were of $V_λ$ origin (data not shown). Three rounds of panning against protein L resulted in enrichment for large plaques. Thirty-four of the large plaques were sequenced and 32 unique sequences were identified (**Fig. 1**). Except for HVLP389, which is from the λ class (subgroup $V_λ$1, V germline 1b), the remaining 31 V_Ls belonged to the $V_κ$ class. Of the 31 κ class V_Ls, 24 fell within the $V_κ$3 subgroup and 7 fell within the $V_κ$1 subgroup. Sixteen of the 24 $V_κ$3 sequences utilized the L6 V germline sequence, while the remaining sequences utilized A27, L2, and L16 V germline sequences. The $V_κ$1 subgroup V_Ls originated from the O2/O12 or A30 V germline sequence. Noticeable mutations occurred at position 96. The germline amino acids at this position are aromatic and hydrophobic amino acids Trp, Phe, Tyr, Leu or Ile for κ class V_Ls, and Tyr, Val or Ala for λ class V_Ls. In the selected pool of κ class V_Ls, however, only 5 out of 31 V_Ls had their germline amino acids at position 96: HVLP325, HVLP349, HVLP388, HVLP3109, and HVLP393; 21 V_Ls had charged amino acids, of which 20 were positively charged, 2 had Pro, 1 had Gln, 1 had Ser, and one had Thr at positions 96. Moreover, 18 V_Ls of the κ class had their last three germline residues (105–107) replaced with amino acids Thr, Val, and Leu, which are only found in λ class V_Ls.

Expression yield and aggregation status of human V_Ls

Eight of the selected V_Ls representing different V germline origins were expressed in *E. coli* TG1 in 1 L cultures and purified: HVLP324, HVLP325, HVLP335, HVLP342, HVLP351, HVLP364, HVLP389, and HVLP3103 (**Fig. 2A**; **Table 1**). All were expressed in good yields ranging from 6.2 mg for HVLP325 to ~75 mg for HVLP335 and HVLP364. The aggregation tendency of the human V_Ls was assessed by Superdex 75™

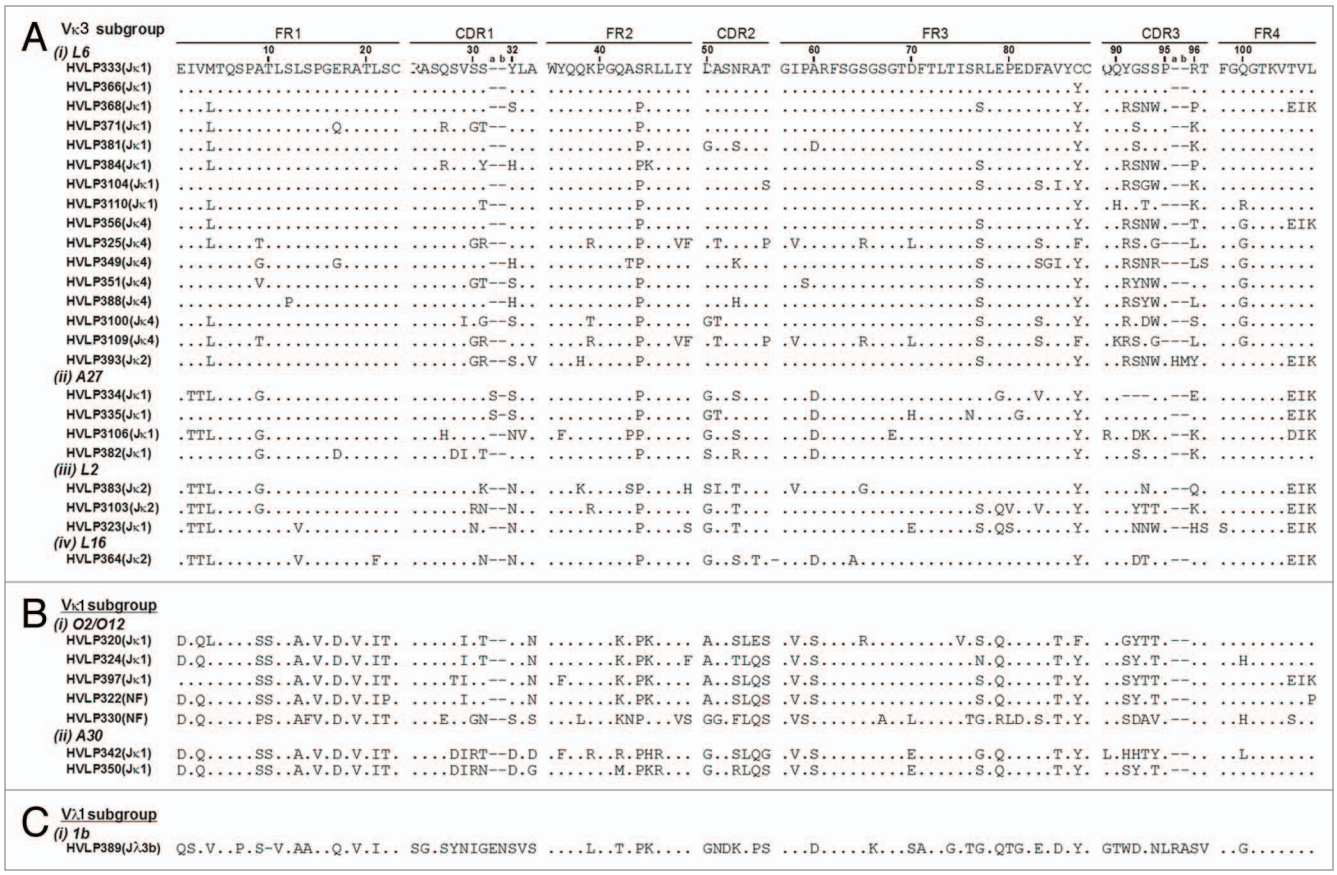

Figure 1. Amino acid sequences of V_Ls selected from a human V_L phage display library by panning against protein L. The dots in the sequence entries indicate amino acid identity with HVLP333. Dashes are included for sequence alignment. See V BASE (http://vbase.mrc-cpe.cam.ac.uk/index.php?&MMN_position=1:1) for sequence numbering and CDR and FR designations. L6, A27, L2, L16, O2/O12, A30, and 1b are V germline gene segment designations. J germline gene segment designations are in brackets. NF, not found.

size-exclusion chromatography (SEC).[47] At a concentration of 0.6 mg/mL (43 μM) all V_Ls were essentially free of aggregates and gave single, symmetrical peaks (**Fig. 3A**). HVLP351, HVLP342, HVLP335 and HVLP3103, were still monomers when tested at their highest concentration available, i.e., 0.89 mg/mL (64 μM), 1.0 mg/mL (72 μM), 4.9 mg/mL (352 μM), and 5.9 mg/mL (430 μM), respectively, although slight tailing was observed for the HVLP335 monomeric peak at 5.9 mg/mL, suggesting V_L interaction with the column matrix. The apparent molecular masses (M_{app}s) of V_Ls, calculated from their elution volumes (**Fig. S1**), ranged from 6.9 kDa to 24.3 kDa, with a mean M_{app} ± SEM of 13.7 ± 2.2 kDa and a M_{for} ± SEM of 13.8 ± 0.04 kDa. Variation in M_{app}s for non-aggregating V_Ls with similar formula molecular masses (M_{for}s) has been reported previously.[32] Such variation was also observed in the case of highly non-aggregating V_Hs and may have been the result of weak transient interactions with the column materials or monomer/dimer equilibria.[53] The non-aggregating status of V_Ls was confirmed by a surface plasmon resonance (SPR) assay based on the Ni^{2+}-His_6 tag interaction that involved flowing His-tagged V_Ls over Ni^{2+}-immobilized sensorchip surfaces.[46] Similar to previous results obtained with monomeric V_Hs, for the two dissociation phase windows tested, all the C-terminally His_6-tagged V_Ls gave k_{off}s that are very similar to those of the monomeric V_HH control, but drastically faster than those for the dimeric V_H control with two C-terminal His_6 tags, confirming the monomeric status of the V_Ls (**Fig. 3B**). This conclusion was accurately endorsed by the multiangle light scattering (MALS) experiments, which showed that the V_Ls had M_{MALS}s (molecular masses determined by MALS) that were very similar to their M_{for}s (**Table 1**).

Protein L binding of human V_Ls

As anticipated, all selected V_Ls bound to protein L in SPR analysis (**Fig. S2A**; **Table 1**). The K_Ds of binding to protein L were in the 0.2–3 μM range, with HVLP324 and HVLP342, which belong to $V_κ1$ subgroup, showing additional smaller K_Ds of 0.07 μM and 0.04 μM, respectively, when Biacore analyses were performed at a low concentration range (1–10 nM) (**Table 1**). The estimated stoichiometry of binding, V_L:protein L, were 7 for $V_κ1$ subgroup members, 3 for all $V_κ3$ subgroup members except for HVLP351 which was 2, and 1 for HVLP389, a $V_λ1$ member.

***T_m*s of human V_Ls**

To assess the thermostability of the V_Ls, T_ms of V_Ls were determined based on ellipticity data assuming a two-state system, which is in agreement with the observed denaturation curves corresponding to a sharp transition into denaturation (**Fig. 4A**).

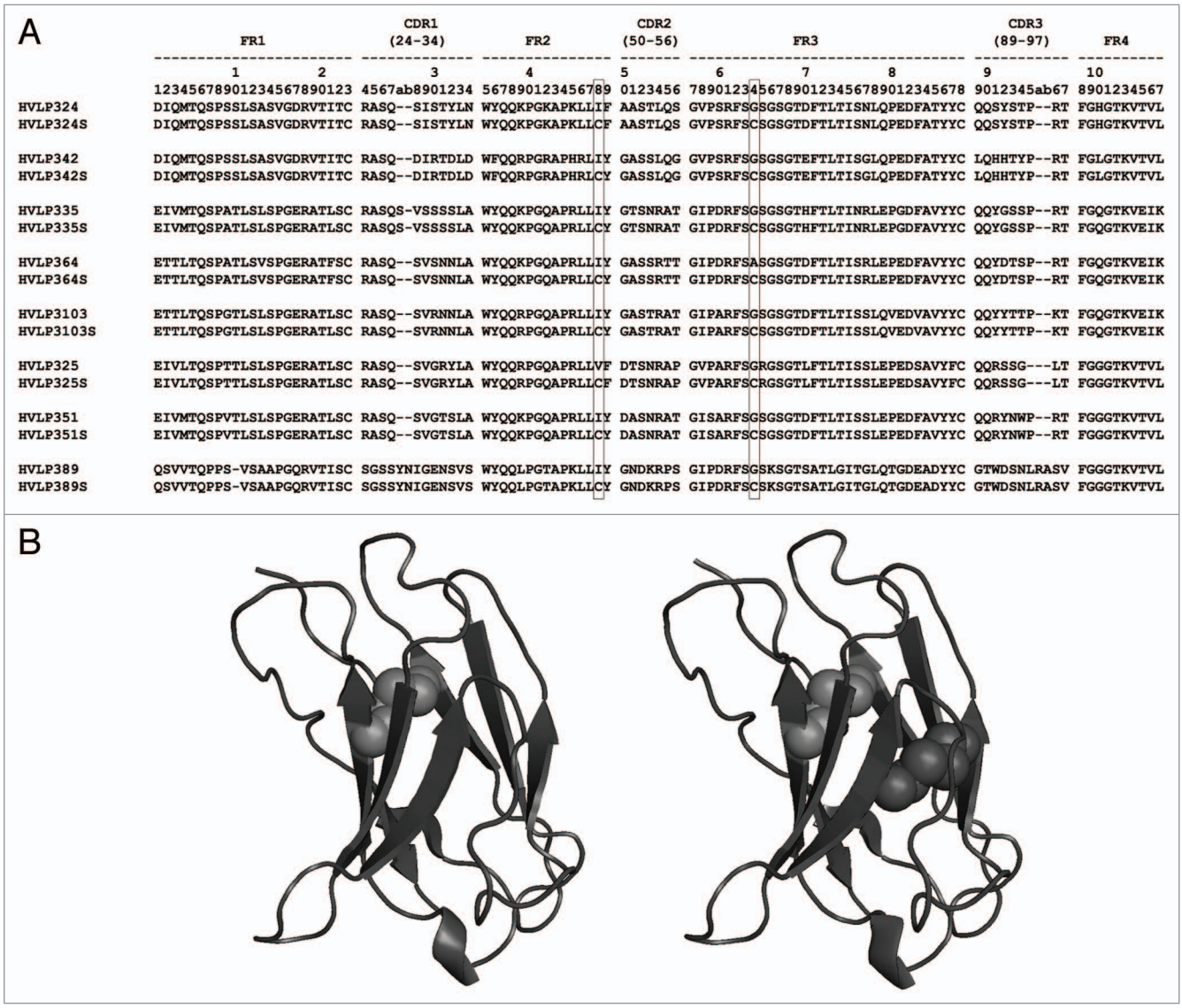

Figure 2. Structure of a set of human V_Ls chosen for detailed biophysical analyses. (**A**) Amino acid sequences of eight human V_Ls and their Cys mutant versions. The amino acid positions (48 and 64) where mutations to cysteine residues were made are marked. (**B**) Homology structures of wild-type (left) and Cys mutant (right) of HVLP324. The native and engineered non-canonical disulfide linkages are shown as light grey and dark grey spheres, respectively. Protein homology structures were obtained using the Geno3D automatic modeling tool (http://pbil.ibcp.fr/htm/index.php). The figures were drawn with PyMOL (www.pymol.org) and Disulfide by Design (version 1.20) freeware.[80]

T_ms, taken at midpoint of the sigmoidal denaturation curves of molar ellipticity change ($\Delta\theta$) vs. temperature (°C), were in the range of 51.9–68.5 °C (median T_m = 61.9 °C) (**Table 1**). The lowest T_m was that of HVLP389, which is the only V_L of λ family among the eight V_Ls, and the highest T_m was that of HVLP325, which showed slight aggregation (**Fig. 3A; Table 1**). The T_ms of eight non-aggregating V_Hs (HVHP428, HVHP413, HVHP414, HVHP421, HVHP429, HVHP44, HVHP420, and HVHP419) isolated previously in the same manner as V_Ls[48] were also determined for comparison. The T_m range was 54.2–64.2 °C and the median T_m was 57.6 °C; the T_m differences between V_Ls and V_Hs were not significant (Mann-Whitney test, two-tailed; P = 0.2345) (**Fig. 4B and D**).

Thermal refolding efficiency of human V_Ls

The ability of the human V_Ls to refold following thermal denaturation was assessed by determining their thermal refolding efficiencies (TREs), which is calculated as the ratio of the K_Ds for the binding of the native V_Ls to protein L (K_Dn) to the K_Ds for the binding of the heat-denatured/cooled (refolded) V_Ls to protein L ($K_D$ref).[48,54] K_Ds were determined by SPR (**Fig. 5**; **Fig. S3**; **Table 1**). **Figures 5A and B** compare the protein L binding sensorgram profiles for HVLP335 and HVLP325, respectively, in native and refolded states at 20 μM V_L concentrations. It can be seen that for HVLP335, with near perfect refolding (95%) (**Table 1**), the sensorgrams for the native and refolded species are almost superimposable. In contrast, for HVLP325 with

Table 1. Biophysical characteristics of V_Ls

V_L	Sub-group	M_{for} (kDa)	M_{MALS} (kDa)[a]	Expression yield (mg)[b]	K_D (μM)	V_L:protein L[c]	T_m (°C)	ΔT_m (°C)	TRE (%)[d]		GI protease resistance (%)[e]		
									4 μM	20 μM	Trypsin	Chymotrypsin	Pepsin
HVLP324	$V_κ1$	13.83	13.84 ± 0.76	2.5, 7	0.2, 0.07[f]	7:1	66.1	7.3	90	78	34	100	22
HVLP324S		13.87	14.68 ± 0.58	0.5, 1.1	0.1, 0.06[f]	7:1	73.4		ND[g]	ND[g]	32	36	46
HVLP325	$V_κ3$	13.61	13.5 ± 0.63	0.5, 6.2	1	3:1	68.5	14	94	65	67	76	34
HVLP325S		13.66	13.35 ± 0.64	2.2, 3.1	1	3:1	82.5		ND[g]	ND[g]	81	93	100
HVLP335	$V_κ3$	13.90	15.26 ± 0.50	73.5	2	3:1	61.7	17.3	92	95	2	59	0
HVLP335S		13.94	16.8 ± 0.47	5.5	2	3:1	79.0		ND[g]	ND[g]	0	32	62
HVLP342	$V_κ1$	13.95	14.22 ± 0.64	1, 7.7	0.6, 0.04[f]	7:1	58.4	5.4	92	70	25	73	3
HVLP342S		13.99	17.02 ± 0.40	1.7, 10.8	0.2, 0.05[f]	7:1	63.8		ND[g]	ND[g]	5	40	5
HVLP351	$V_κ3$	13.85	14.60 ± 0.61	1.2, 8.9	2	2:1	62.0	9.9	87	65	71	100	31
HVLP351S		13.89	14.61 ± 0.53	1.9, 4.8	0.7	2:1	71.9		ND[g]	ND[g]	100	99	94
HVLP364	$V_κ3$	13.95	14.20 ± 0.58	0.3, 77	3	3:1	57.0	15.3	100	92	32	58	0
HVLP364S[h]		13.97	14.98 ± 0.43	4.7	ND[g]	ND[g]	72.3		ND[g]	ND[g]	0	12	0
HVLP3103	$V_κ3$	13.85	14.29 ± 0.64	0.7, 19	1	3:1	65.7	10.7	94	92	81	90	0
HVLP3103S		13.89	14.05 ± 0.68	6.5	1	3:1	76.4		ND[g]	ND[g]	47	80	89
HVLP389	$V_λ1$	13.69	15.12 ± 0.50	3, 16.7	1	1:1	51.9	14.4	91	91	15	74	0
HVLP389S		13.72	13.65 ± 0.68	6.5	1	1:1	66.3		ND[g]	ND[g]	64	90	11

[a]Mean ± SEM; [b]Expression yield values are per liter of bacterial culture. Two expression yield values correspond to two independent expression trials; [c]Stoichiometry of V_L-protein L binding; [d]Thermal refolding efficiency at 4 and 20 μM V_L concentrations, respectively; [e]Percentage proteolytic resistance values are at protease concentrations of 10 μg/mL (see also **Fig. 6E**); [f]Smaller K_D values correspond to the binding of HVLP324, HVLP324S, HVLP342, and HVLP342S to the high affinity sites on protein L; [g]ND, not determined; [h]HVLP364S additionally gave a significant second peak (**Fig. 3A**) with a smaller elusion volume and a M_{MALS} of 26.21 ± 0.47 kDa.

65% TRE (**Table 1**), a significant drop in binding is observed for refolded species compared with the native species when sensorgrams at the same concentrations are compared. At 4 μM V_L concentrations, TREs are in the range of 90–100%, except for HVLP351, which is slightly lower at 87%, indicating a near perfect refolding for V_Ls (median = 92%) (**Fig. 5C**). At 20 μM V_L concentrations, the TREs significantly decrease, with V_Ls having a TRE range of 65–95% and a TRE median dropping to 84.5% (Wilcoxon matched-pairs signed rank test, two-tailed; P = 0.0469) (**Fig. 5C**). However, for four V_Ls (HVLP335, HVLP364, HVLP389, HVLP3103), TRE values still remains above 90%, and for three of the four, TREs do not change when V_L concentrations are increased from 4 μM to 20 μM. For comparison, the TREs of the eight non-aggregating V_Hs at 4 μM and 20 μM V_H concentrations are also included (**Fig. 5C**; **Fig. S4**). Two of the eight V_Hs (HVHP428 and HVHP413) showed low TREs of 48% and 7% at 4 μM, with the remaining 6 V_Hs (HVHP414, HVHP421, HVHP429, HVHM44, HVHP420, HVHP419) having TREs of 90–98% (median = 92%). As with V_Ls, the TREs of V_Hs at 20 μM concentrations decreased significantly (median = 78.5%, Wilcoxon matched-pairs signed rank test, two-tailed; P = 0.0078), with HVHP428 and HVHP413 V_Hs failing to refold (TRE = 2% and 1%, respectively). Statistical analysis of TREs revealed that V_Ls were comparable to V_Hs in terms of reversibility of thermal unfolding [Mann-Whitney test, two-tailed; P = 0.8785 (4 μM), P = 0.5054 (20 μM)]. Moreover,

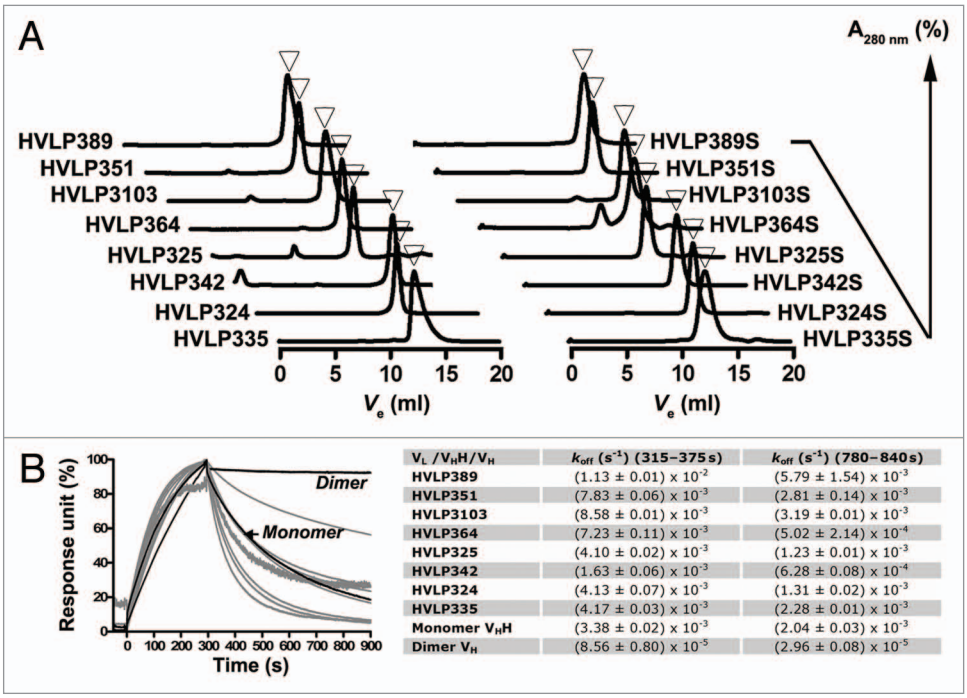

V_L /V_HH/V_H	k_{off} (s^{-1}) (315–375 s)	k_{off} (s^{-1}) (780–840 s)
HVLP389	(1.13 ± 0.01) x 10^{-2}	(5.79 ± 1.54) x 10^{-3}
HVLP351	(7.83 ± 0.06) x 10^{-3}	(2.81 ± 0.14) x 10^{-3}
HVLP3103	(8.58 ± 0.01) x 10^{-3}	(3.19 ± 0.01) x 10^{-3}
HVLP364	(7.23 ± 0.11) x 10^{-3}	(5.02 ± 2.14) x 10^{-4}
HVLP325	(4.10 ± 0.02) x 10^{-3}	(1.23 ± 0.01) x 10^{-3}
HVLP342	(1.63 ± 0.06) x 10^{-3}	(6.28 ± 0.08) x 10^{-4}
HVLP324	(4.13 ± 0.07) x 10^{-3}	(1.31 ± 0.02) x 10^{-3}
HVLP335	(4.17 ± 0.03) x 10^{-3}	(2.28 ± 0.01) x 10^{-3}
Monomer V_HH	(3.38 ± 0.02) x 10^{-3}	(2.04 ± 0.03) x 10^{-3}
Dimer V_H	(8.56 ± 0.80) x 10^{-5}	(2.96 ± 0.08) x 10^{-5}

Figure 3. Size-exclusion chromatography and SPR analyses of wild-type and mutant V_Ls. (**A**) Superdex 75™ size-exclusion chromatograms of V_Ls with monomeric peaks marked with arrowheads. For HVLP364S, the dimeric V_L peak situated to the left of the monomeric peak is visible. (**B**) SPR analysis of V_L binding to a Ni^{2+}-NTA sensorchip. A llama V_HH Monomer (A4.2[49]) and a V_H Dimer[81] were used as controls. Measurements were taken at two dissociation phase windows (315–375 s and 780–840 s) and the mean values obtained from two independent trials performed in duplicates were recorded in the table. SPR experiments were performed with SEC-purified V_Ls.

the drops in TRE values as a function of increased concentrations of V_Hs and V_Ls are significant and expected as previously reported.[55] No significant correlation between TRE and T_m was found.

Protease resistance of human V_Ls

In addition to thermostability, e.g., T_m, protease resistance is also a measure of protein stability. To determine protease resistance, V_Ls were treated with major gastrointestinal (GI) proteases, trypsin, chymotrypsin, and pepsin, at various protease concentrations (**Fig. 6**; **Table 1**). As expected, a gradual decrease in protease resistance of V_Ls was observed as a function of protease concentration for all three proteases (**Fig. 6A, B, and C**). At the highest trypsin concentration (20 μg/mL), the protease resistance of V_Ls was in the range of 0–75% with a median resistance of 16% (**Fig. 6A**). The V_Ls, however, demonstrate higher resistance to chymotrypsin (**Fig. 6B**). For example, the V_Ls demonstrated a median resistance of 75% at a chymotrypsin concentration of 10 μg/mL compared with 33% for trypsin at the same concentration; at a higher chymotrypsin concentration of 20 μg/mL, V_Ls had a protease resistance range and median of 34–100% and 67.5%, respectively. V_Ls showed the least resistance to pepsin (**Fig. 6C**). At 1 μg/mL pepsin concentration, two of the V_Ls (HVLP364 and HVLP389) were digested almost completely with 8% and 2% pepsin resistance, respectively, and at 10 μg/mL pepsin concentration, the resistance of all V_Ls decreased to below 34% (median resistance = 1.5%) (**Table 1**). At 20 μg/mL pepsin concentration, the pepsin resistance range and median were 0–23% and 0%, respectively.

We compared V_Ls to the eight non-aggregating V_Hs in terms of resistance to the three proteases at 10 μg/mL protease concentration (**Fig. 6D**). We found that there was no significant difference between V_Ls and V_Hs with respect to resistance to trypsin (Mann-Whitney test, two-tailed; P = 0.1605). V_Ls were significantly more resistant to chymotrypsin than V_Hs (Mann-Whitney test, two-tailed; P = 0.0148), while the opposite was true with respect to resistance to pepsin (Mann-Whitney test, two-tailed; P = 0.0011). Theoretical numbers of protease cleavage sites were determined by a protease digestion prediction webware (http://web.expasy.org/peptide_cutter). It was found that V_Hs had significantly higher number of protease cleavage sites than V_Ls for all three proteases [trypsin sites medians: 8.5 and 10.5 for V_L and V_H, respectively, (Mann-Whitney test, two-tailed; P = 0.0207); chymotrypsin sites medians: 10 and 13.5 for V_L and V_H, respectively, (Mann-Whitney test, two-tailed; P = 0.0070); pepsin sites medians: 30 and 39.5 for V_L and V_H, respectively [Mann-Whitney test, two-tailed; P = 0.0002)].

Disulfide linkage engineering of human V_Ls

To improve the stability of human V_Ls, we created 8 V_L mutants (HVLP324S, HVLP325S, HVLP335S, HVLP342S, HVLP351S, HVLP364S, HVLP389S, and HVLP3103S) with a pair of Cys substitutions at amino acid positions 48 and 64 (**Fig. 2A**). All were expressed well in *E. coli*, albeit with lower yields compared with wild-type V_Ls, with expression yields ranging from 1.1 mg/L of bacterial culture in shaker flasks for HVLP324S to ~11 mg/L for HVLP342S (**Table 1**).

To determine if the engineered Cys pairs formed the desired disulfide linkages in the mutants, mass spectrometry (MS) was performed by analyzing tryptic digests of mutant V_Ls. The MS analyses revealed that the disulfide linkage was formed as intended in all V_L mutants (**Fig. S5**; **Table 2**). The disulfide-linked peptide ions appeared prominent in the survey of LC-MS chromatograms with tryptic peptides of the mutant V_Ls. The expected disulfide-linked peptide sequences corresponding to each mutant V_Ls were confirmed by manual de novo sequencing. When there was only one disulfide linkage between two peptides, the exact disulfide linkage position was confirmed by an almost complete disulfide-linked y fragment ion series from one peptide with the other peptide attached as a modification via a disulfide bond that remains intact under collision-induced dissociation

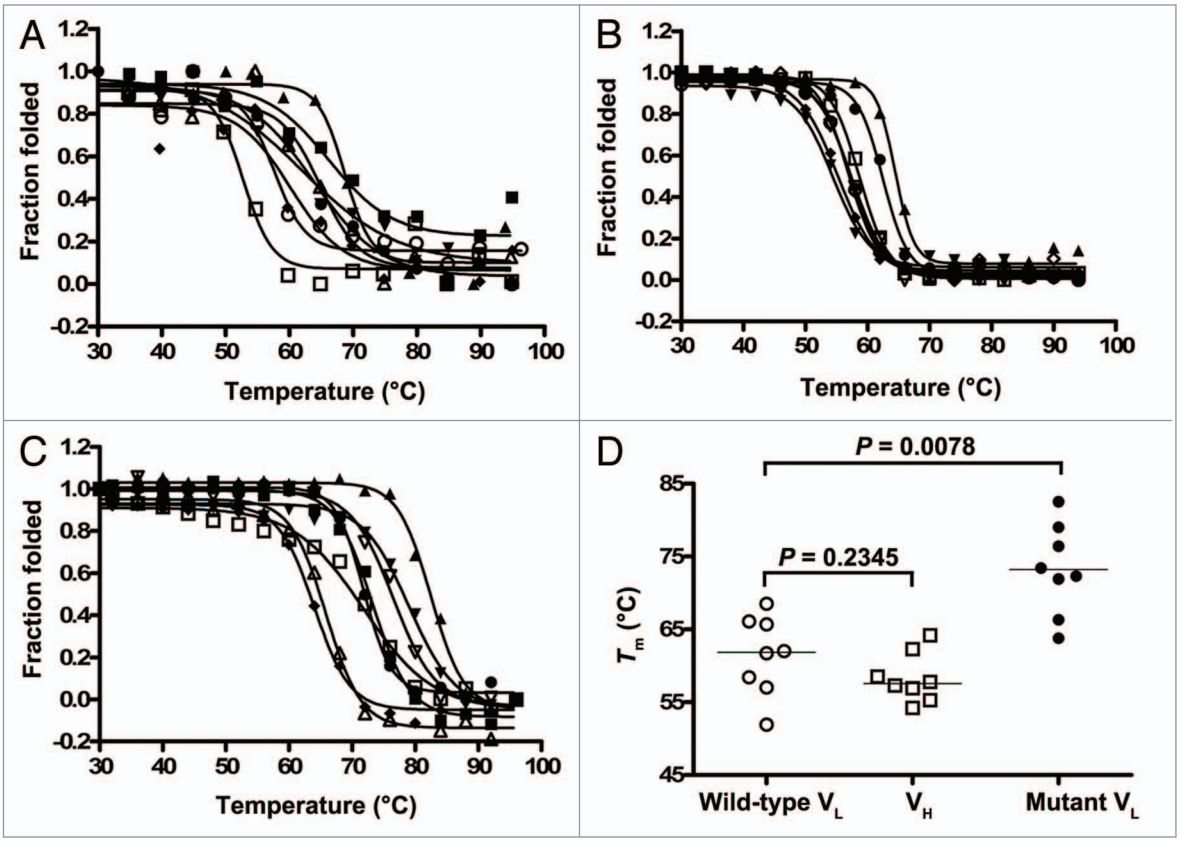

Figure 4. Thermostability analysis of antibody domains. Thermal unfolding curves of (**A**) wild-type V_Ls, (**B**) V_Hs, and (**C**) mutant V_Ls. T_ms were calculated and incorporated into **Figure 4D** and **Table 1**. The non-aggregating V_Hs are described in ref. 48. (**D**) Graph comparing the T_ms of wild-type V_Ls to those of V_Hs and mutant V_Ls.

(CID),[47,49,56] e.g., the disulfide linked peptides ATLSCR (P1) and GSGTLFTLTISSLEPEDSAVYFCQQR (P2) of HVLP325S (**Table 2**; MS^2 data not shown). When there were three peptides linked by two disulfide bonds, the y fragment ion containing the linkage close to the N-terminal of two peptides was difficult to observe. Nevertheless, an almost complete y ion series of each peptide was observed. For example, a prominent ion at m/z 1042.66 (6+) from HVLP324S tryptic disulfide-linked peptide LLCFAASTLQSGVPSR (P1), FSCSGSGTDFTLTISNLQPEDFATYYCQQSYSTPR (P2) and VTITCR (P3) was observed from the survey of LC-MS chromatogram (**Fig. S5B** (top panel); **Table 2**). Informative y fragment ions were observed from P2 with P3 as a modification via a disulfide bond, and an almost complete y ion series of P1 was observed as well (**Fig. S5B**, top panel). To further confirm the above disulfide bond formation in the mutant HVLP324S, the electron transfer dissociation (ETD)-MS^2 spectrum of the peptide ion $[M + 5H]^{5+}$ at m/z 1250.99 (5+) from the same disulfide-linked peptide of HVLP324S was acquired (**Fig. S5B**, middle panel). The most abundant charge-reduced ETD fragment ion $[M + 5H]^{4+\bullet}$ at m/z 1563.49 (4+) was selected for CID to obtain the ETD-CID-MS^3 spectrum of the m/z 1250.99 (5+) ion (**Fig. S5B**, bottom panel). The intact P1, P2, and P3 ions at m/z 691.47 (1+), 1648.86 (1+), and 1956.85 (2+), respectively, were all observed at relatively high abundances upon dissociation of the disulfide linkages of the three linked peptides by ETD. Tryptic peptides linked by the engineered disulfide bonds were positively identified for all mutant V_Ls. These fragments are recorded in **Table 2**.

Aggregation status of disulfide linkage-engineered human V_Ls

Next, we aimed to determine if the engineered disulfide linkage compromised the non-aggregation status of V_Ls. To this end, we assessed the mutant V_Ls by Superdex 75™ SEC. Except for HVLP364S, which seemingly formed dimeric aggregates at ~17%, the remaining seven V_L mutants were monomeric (**Fig. 3A**), indicating that similar to wild-type V_Ls, mutant V_Ls with the extra disulfide linkage were aggregation-resistant. Moreover, the slight aggregation observed in HVLP325 disappeared in the mutant version, HVLP325S. The M_{app}s of mutant V_Ls, calculated from their elution volumes, were similar to those of wild-type versions, ranging from 4.9 kDa to 23.5 kDa with a mean M_{app} ± SEM of 11.4 ± 2.3 kDa compared with 13.7 ± 2.2 kDa for the wild-type V_Ls. The SEC results were further confirmed by the MALS data, which showed that the V_Ls were indeed monomeric as their experimental M_{MALS}s were very close to their theoretical M_{for}s (**Table 1**). Furthermore, the minor HVLP364S peak identified as corresponding to a V_L dimer in

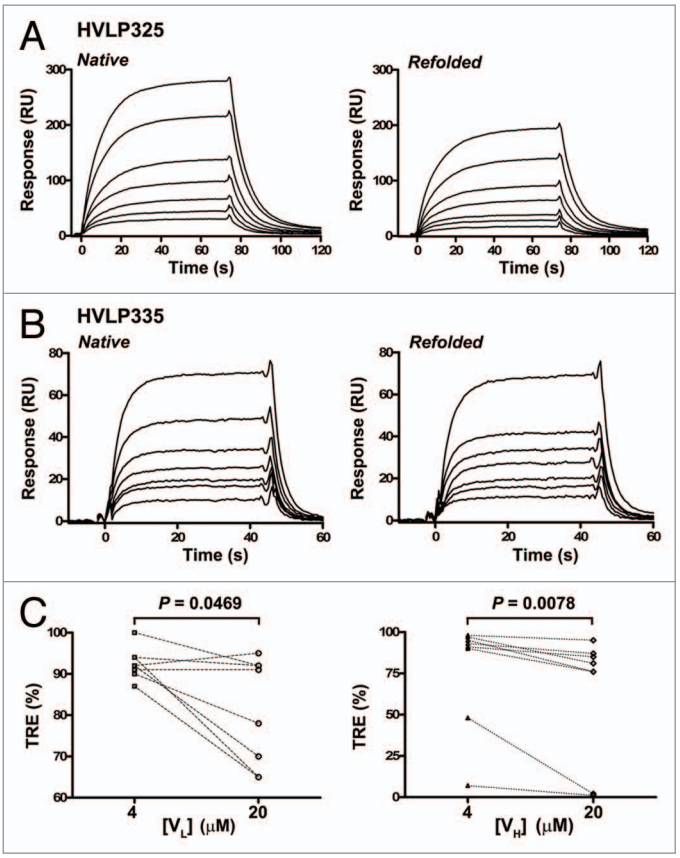

Figure 5. Thermal refolding efficiency determination of human V_Ls and V_Hs by SPR. (**A**), (**B**) Representative SPR sensorgrams for the binding of native and heat-denatured/cooled (refolded) human V_Ls to immobilized protein L. Data are from TRE experiments performed at 20 μM V_L concentrations. V_L concentrations used to construct each sensorgram set was 12.5, 18.8, 25, 37.5, 50, 75, and 100 nM for HVLP325 and 12.5, 20, 25, 30, 38, 50, and 75 nM for HVLP335. See **Figure S3 and S4** for SPR data for all V_Ls and V_Hs. The $K_D$ns and $K_D$refs determined from "Native" and "Refolded" sensorgram pairs were used to determine TREs in (**C**). (**C**) TREs of wild-type V_Ls and V_Hs obtained under 4 μM and 20 μM domain concentration conditions in refolding experiments. Lines connect TREs for the same clones.

SEC had indeed the M_{MALS} for a dimeric V_L: 26.21 ± 0.47 kDa (vs. the expected M_{for} of 27.94 kDa).

Probing conformational changes in disulfide linkage-engineered human V_Ls by protein L binding

To probe any possible structural changes brought about by the non-canonical disulfide linkage in V_L mutants, the binding of V_L mutants to protein L was quantified by SPR. We found that all V_L mutants, with the exception of HVLP324S, HVLP342S, and HVLP351S, bound to protein L with almost the same K_Ds (and k_{on}s and k_{off}s) as their wild-type counterparts (**Fig. S2**; **Table 1**), indicating that, for the majority of V_Ls, there were no structural changes due to the engineered disulfide linkage, or if there were any, they were too subtle to be sensed by protein L. HVLP324S, HVLP342S and HVLP351S showed 2- to 3-fold affinity increase toward protein L low affinity binding sites compared with wild-type counterparts. In contrast, in all cases the stoichiometry of V_L:protein L binding remained unchanged between the wild-type and corresponding mutant V_Ls. In the case of HVLP364S, the K_D seemed to be in the low micromolar range, but a reliable K_D, and consequently a reliable stoichiometry, could not be determined by SPR due to aggregate contamination in the V_L sample. A homology structure of HVLP324S suggests that the non-canonical disulfide linkage and protein L binding site occupy distinct locations in mutant V_Ls (**Fig. 7**). In contrast, for a V_H with a similar disulfide linkage mutation, the non-canonical disulfide linkage is very intimate with and imbedded within the protein A binding site (**Fig. 7**).

Thermal stability of disulfide linkage-engineered human V_Ls

To determine the effect of the non-canonical disulfide linkage on the thermal stability of V_Ls, the T_ms of mutant V_Ls were determined and compared with those for wild-type V_Ls. The T_ms were in the range of 63.8–82.5 °C (median T_m = 72.9 °C) compared with 51.9–68.5 °C (median T_m = 61.9 °C) for wild-type V_Ls (**Fig. 4C and D**; **Table 1**). The thermostability improvements were significant, reflecting a T_m increase (ΔT_m) range and median of 5.4–17.3 °C and 12.4 °C, respectively (**Fig. 4D**; **Table 1**) (Wilcoxon matched-pairs signed rank test, two-tailed; P = 0.0078). Although the result indicated that the engineered disulfide linkage stabilized the V_Ls regardless of their germline subtypes (κ or λ), the thermostability improvements were more pronounced for the κ3 and λ1 subgroup members compared with the κ1 subgroup members.

GI protease resistance of disulfide linkage-engineered human V_Ls

Previously, V_HHs were shown to have acquired protease resistance with the addition of a similar non-canonical disulfide linkage.[49] We therefore investigated the effect of the non-canonical disulfide linkage on the resistance of V_Ls to trypsin, chymotrypsin, and pepsin. Mutant V_Ls were digested with varying concentrations of proteases under the same digestion conditions as for wild-type V_Ls (**Fig. 6**). We observed that there was no significant overall difference between wild-type and mutant V_Ls with respect to resistance to trypsin or chymotrypsin (**Fig. 6A, 6B, and 6E**; Wilcoxon matched-pairs signed rank test, two-tailed; P = 0.2969, 0.8438, 0.8438, and 1.0625 for trypsin at 1 μg/mL, 5 μg/mL, 10 μg/mL, and 20 μg/mL, respectively; P = 0.0625, 0.1563, 0.1484, and 0.0781 for chymotrypsin at 1 μg/mL, 5 μg/mL, 10 μg/mL, and 20 μg/mL, respectively).

Mutant V_Ls, however, showed improved resistance to pepsin. The pepsin resistance medians of wild-type V_Ls were 73% and 1.5% at enzyme concentrations of 1 μg/mL and 10 μg/mL, respectively, and decreased to 0% at the concentration of 20 μg/mL (**Fig. 6C**). In contrast, mutant V_Ls had pepsin resistance medians of 100%, 54%, 39.5%, and 25.9% at enzyme concentrations of 1, 10, 20, and 50 μg/mL, respectively. The pepsin resistance improvements were significant at 1 and 10 μg/mL enzyme concentrations (**Fig. 6E**; Wilcoxon matched-pairs signed rank test, two-tailed; P = 0.0078 and 0.0156, respectively), but not so at 20 and 50 μg/mL enzyme concentrations (p = 0.0625 for both concentration conditions). Moreover, the correlation between protease resistance and T_m was explored (**Fig. 6F**). It was found that in general, V_Ls with higher T_ms had higher resistance to pepsin

(Pearson's correlation, 0.6077; P = 0.0125, r^2 = 0.3693, at 1 μg/mL enzyme concentration; Pearson's correlation, 0.7807; P = 0.0004, r^2 = 0.6095, at 10 μg/mL enzyme concentration; Pearson's correlation, 0.7438; P = 0.0010, r^2 = 0.5532, at 20 μg/mL enzyme concentration; Pearson's correlation, 0.6837; P = 0.0035, r^2 = 0.4674, at 50 μg/mL enzyme concentration). No significant correlation was observed in the case of trypsin or chymotrypsin (data not shown).

Discussion

Numerous publications in the past two decades have firmly established the suitability of sdAbs as therapeutic and diagnostic agents. Human V_H and V_L sdAbs, in particular, have been pursued as therapeutics due to their expected lower immunogenicity in patients compared with other classes of sdAbs such as camelid V_HHs and shark V_{NAR}s.[4,5,32] A number of studies have highlighted V_Ls as bona fide affinity reagents, and a few, in particular, have pointed to an inherent property of V_Ls as being more aggregation resistant than V_Hs.[23,32-34,57-61] Thus, from the aggregation point of view, human V_Ls may be preferable over human V_Hs as immunotherapeutics. In this study, we set out to obtain a deeper understanding of V_Ls with respect to a number of biophysical properties, including their aggregation tendencies.

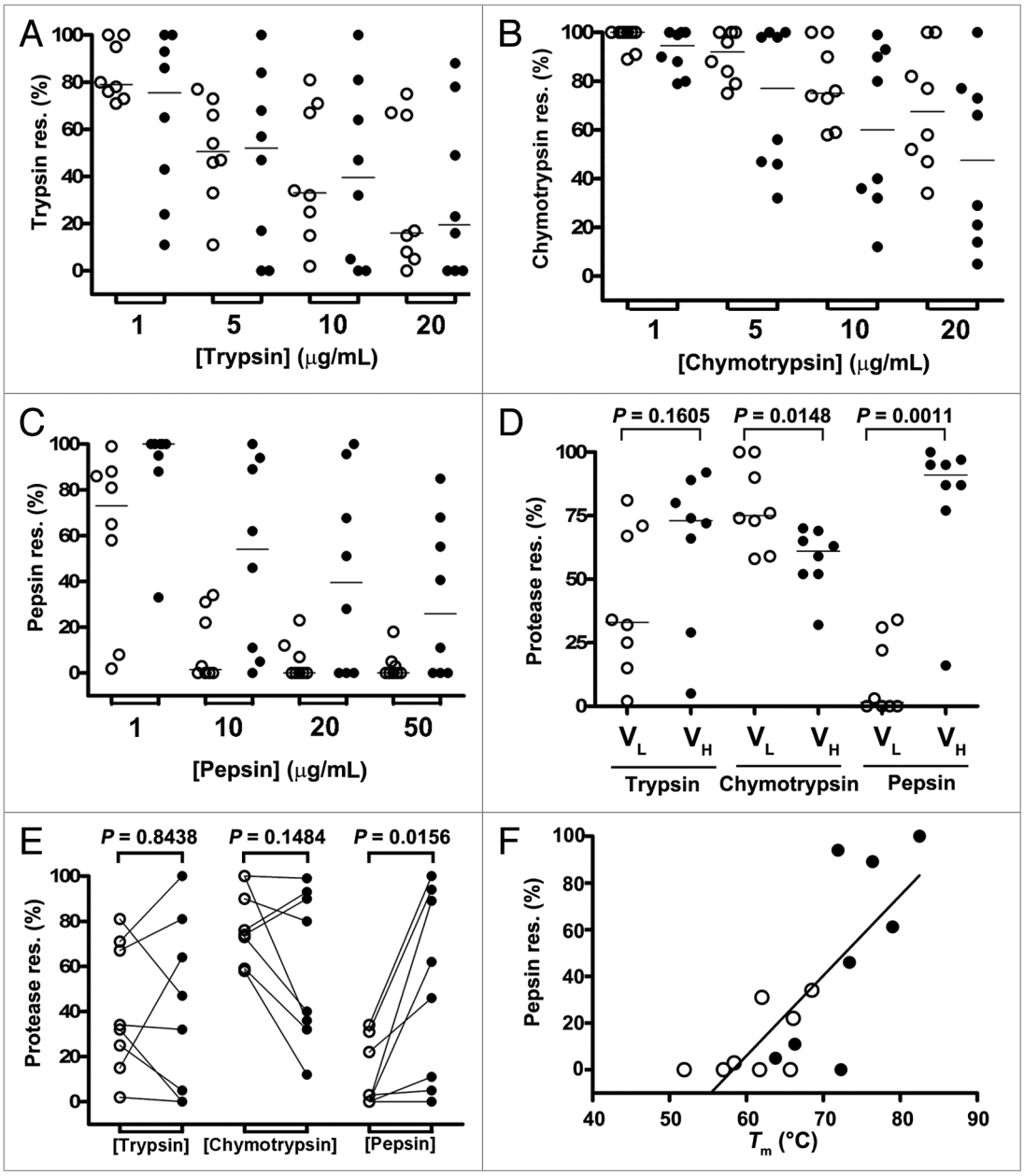

Figure 6. GI protease resistance profiles for human V_Ls and V_Hs. (**A**), (**B**), (**C**) Trypsin, chymotrypsin, and pepsin resistance (res.) of human V_Ls (open circles) and their corresponding Cys mutants (closed circles). (**D**) Graph comparing V_Ls to V_Hs in terms of resistance to trypsin, chymotrypsin, and pepsin at 10 μg/mL protease concentrations. Horizontal lines in graphs (**A**)–(**D**) represent medians. (**E**) Graph showing trypsin, chymotrypsin, and pepsin resistance of human V_Ls (open circles) and their corresponding Cys mutants (closed circles) in pair-wise manner at 10 μg/mL protease concentrations (*see* also **Table 1**). Lines connect protease resistances value for each V_L to that for its corresponding mutant version. The p values in graphs (**D**) and (**E**) were obtained by the Mann-Whitney test (two-tailed) and Wilcoxon matched-pairs signed rank test (two-tailed), respectively, using GraphPad Prism (GraphPad Software). (**F**) A correlation graph of pepsin resistance *vs.* T_m (Pearson's correlation, 0.7807; p = 0.0004, r^2 = 0.6095). Data are from digestion experiments performed at 10 μg/mL pepsin concentrations. Open circles, wild-type V_Ls; closed circles, mutant V_Ls.

Human V_H domains are known for their general tendency to aggregate. Previously, a phage selection method was used to obtain exclusively non-aggregating human V_H domains from a naïve human V_H phage display library that was propagated as plaques.[48] The library, with a size of 6 × 10^8 transformants, was panned against the B cell super-antigen protein A, and sequencing of more than 110 clones with complete V_H open reading frames yielded a total of 15 non-aggregating V_Hs. By applying

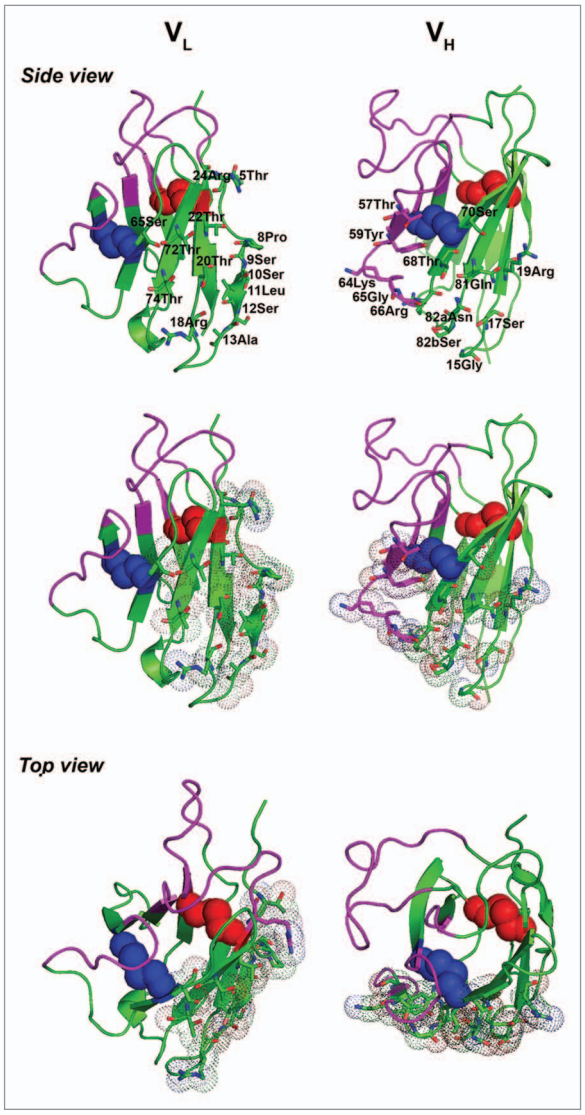

Figure 7. Homology structures of HVLP324S V_L and huVHAm302S V_H, comparing the positioning of protein L binding site to protein A binding site relative to the engineered non-canonical disulfide linkages (blue spheres) for the V_L and V_H, respectively. huVHAm302S is a previously described human V_H that lost its protein A binding activity by 3.5-fold upon the introduction of a non-canonical disulfide linkage at positions 49 and 69.[46] Red spheres represent the native, canonical disulfide linkage, pink- and green-colored regions CDRs and FRs, respectively. Amino acid residues forming protein L binding sites 1 and 2 (top, left panel) and protein A binding site (top, right panel) are shown. The binding site residues were identified based on the published crystal structures of the complex between a human antibody Fab fragment (2A2, κ1 subtype, V_H3 family) and a single *Peptostreptococcus magnus* protein L domain[64] (V_L) and between Fab 2A2 and domain D of *Staphylococcus aureus* protein A[82] (V_H). Middle and bottom panels show side and top views of the protein L and protein A binding sites in dots and sticks presentations. Protein homology structures were obtained as described in the **Figure 2** legend. The figures were drawn with PyMOL (http://www.pymol.org) and manipulated using Adobe Photoshop CS2 software.

essentially the same selection approach, we obtained a total of 32 unique sequences out of 34 screened clones from a 200-fold smaller-sized V_L library. Given that the selection method has been shown to select only for non-aggregating domains, this high yield isolation of V_Ls implies that human V_Ls are more frequently aggregation resistant than human V_Hs, which is consistent with previous findings.[32,33] This is further supported by the fact that our subset of randomly selected protein L binding V_Ls representing different germline origins were indeed non-aggregating as shown by size-exclusion chromatography, hexa-histidine capture SPR and multiangle light scattering experiments. This also confirms the power of the aforementioned selection approach for the isolation of non-aggregating proteins. However, an intrinsic ability of protein L to screen out structurally compromised, aggregating domains in favor of non-aggregating protein L binders during panning experiments is a possibility that may have contributed to the strong selective power of the approach.

It is not surprising that from a library consisting mostly of V_λ class V_L domains, the vast majority of the protein L binding V_Ls isolated (31 out of 32 unique sequences) were of V_κ type ($V_\kappa3$ and $V_\kappa1$ subgroups) with only one being of a V_λ type (HVLP389). Previous studies have shown that protein L predominantly binds to the V_κ type domains, specifically to those in the subgroups $V_\kappa1$, $V_\kappa3$, and $V_\kappa4$, with a paucity of binding to λ class V_Ls.[40,41,62-66] Given the selective nature of our approach for stable (non-aggregating) domains, the predominance of $V_\kappa3$ subgroup type V_Ls (24/31) followed next by $V_\kappa1$ subgroup type V_Ls (7/31), and the absence of any $V_\kappa4$ subgroup type V_Ls, in the pool of selected binders may be a reflection of the relative stability of V_Ls. Previously, it was shown that of the four V_L domains representing the consensus sequences of human subgroups $V_\kappa1$–4, the $V_\kappa3$ V_L was the most thermodynamically stable followed by the $V_\kappa1$ V_L, with the $V_\kappa4$ V_L appearing to be the least stable of the three.[33] Also, unlike the first two V_Ls, which were monomeric, the $V_\kappa4$ V_L formed dimers, an indication of its aggregation tendency.[33] In fact, a bleak selection for the V_λ class V_Ls in this study may not have been just the result of their general lack of binding to protein L, but also the result of their lower stability compared with V_κ class V_Ls.[33] Consistent with this is the fact that our lone λ class binder belongs to the $V_\lambda1$ subgroup, a subgroup whose one representative was shown to be more thermodynamically stable than two other V_Ls representing subgroups $V_\lambda2$ and $V_\lambda3$. It is also possible, however, that the relative proportion of $V_\kappa3$ and $V_\kappa1$ binders may simply reflect their relative proportions in the original, unselected V_L library.

Mutations with respect to V_L germline sequences were observed for the pool of selected V_Ls, but, in the absence of mutational studies, it is very difficult to assign solubility roles to mutation positions. Significant mutations at position 96, e.g., mutations from a hydrophobic germline amino acid to a positively-charged amino acid in the vast majority of V_Ls, including 6 of the 8 non-aggregating, representative V_Ls, suggest a solubility role for position 96. Consistent with this, previous studies with immunoglobulin κ1 light chains have suggested that while an aromatic or hydrophobic residue at position 96 enhances dimerization, a charged amino acid (Arg) at the same position results in stable light chain monomers.[67] It was explained that Arg-Arg charge repulsion at positions 96 of monomers would interfere with dimer formation.[67] Further mutational studies are requireto

Table 2. Disulfide linkage determination of V_Ls by MS analyses

V_Ls	Tryptic peptides[a]	M_{for} (Da)	M_{exp} (Da)	ΔM[c] (Da)
HVLP324S	VTIT**C**R...LL**C**FAASTLQSGVPSR... FS**C**SGSGTDFTLTISNLQPEDFATYY**C**QQSYSTPR	6249.91[b]	6249.96[b]	-0.05[b]
HVLP325S	ATLS**C**R...GSGTLFTLTISSLEPEDSAVYF**C**QQR	3495.66	3495.56	0.10
	LL**C**FDTSNR...FS**C**R	1576.71[b]	1576.68[b]	0.03[b]
HVLP335S	LL**C**YGTSNR...FS**C**SGSGTHFTLTINR	2750.29[b]	2750.32[b]	-0.03[b]
	ATLS**C**R...LEPGDFAVYY**C**QQYGSSPR	2826.27	2826.20	0.07
HVLP342S	VTIT**C**R...L**C**YGASSLQGGVPSR...FS**C**SGSGTEFTLTI SGLQPEDFATYY**C**LQHHTYPR	6136.85[b]	6136.80[b]	0.05[b]
HVLP351S	ATLS**C**R...LL**C**YDASNR... FS**C**SGSGTDFTLTISSLEPE DFAVYY**C**QQR	5049.26[b]	5049.00[b]	0.26[b]
HVLP364S	LL**C**YGASSR...FS**C**SGSGTDFTLTISR	2644.23[b]	2644.32[b]	-0.09[b]
	ATFS**C**R...LEPEDFAVYY**C**QQYDTSPR	3004.29	3004.35	-0.06
HVLP389S	LL**C**YGNDK...FS**C**SK	1492.65[b]	1492.59[b]	0.06[b]
	VTIS**C**SGSSYNIGENSVSWYQQLPGTAPK… SGTSAT LGITGLQTGDEADYY**C**GTWDSNLR	6221.84	6221.97	-0.13
HVLP3103S	ATLS**C**R…LL**C**YGASTR…FS**C**SGSGTDFTLTISSLQV EDVAVYY**C**QQYYTTPK	5528.56[b]	5528.52[b]	0.04[b]

[a]Major tryptic peptides containing disulfide linkages are shown, with connecting cysteine residues single or double underlined (native or engineered Cys (C), respectively) and boldfaced (see **Fig. S5** for experimental details). The triple dots between peptides denote sequence discontinuity, which was caused by the loss of V_L sequences after trypsin digestion; the discontinuing peptides, however, are held together by disulfide linkage(s); [b]The very close match between M_{for} (formula molecular mass) and M_{exp} (experimental molecular mass) indicates the presence of the Cys48-Cys64 disulfide linkage. [c]$\Delta M = M_{for} - M_{exp}$. In addition, the disulfide linkages were confirmed by de novo sequencing the CID or ETD spectra of the disulfide linked peptides (e.g., see **Fig. S5B**).

determine if the presence of a positively-charged amino acid at position 96 leads to V_Ls that are more aggregation resistant, and if so, whether a negatively-charged amino acid would have the same effect. Other studies with immunoglobulin V_H domains showed that substitution with negatively-charged amino acids, Asp substitution in particular, were more effective than positively-charged substitutions in increasing the aggregation resistance of V_Hs.[68]

We also observed that at FR4 positions 105, 106, and 107, instead of the typical Asp/Glu, Ile, and Lys, the majority of the κ class V_Ls had Thr, Val, and Leu, amino acids, respectively, which are characteristic of λ class V_Ls. Whether the substitutions have a role in improving the biophysical properties of the κ class V_Ls remains to be seen. The importance of FR4 residues in improving the aggregation resistance of immunoglobulin variable domains (V_HHs and V_Hs) has been suggested.[69,70] For example, V_HHs, which are known for their high aggregation resistance, have a highly conserved 105Q mutation compared with the aggregation prone V_Hs. Similarly, V_Hs with the 105Q mutation have been shown to have improved aggregation resistance compared with a corresponding wild-type V_H. Also, the role of J segment, which codes for the FR4 amino acids, in increasing the thermal stability and non-aggregation of V_HHs has been shown by others.[69]

SPR binding experiments on the eight representative non-aggregating V_Ls confirmed their protein L binding activity. Of interest were the two $V_κ1$ type binders, which unlike the $V_κ3$ and $V_λ$ type V_Ls that bound to protein L with similar micromolar affinities (1–3 μM), bound to protein L with low (0.2 μM and 0.6 μM) and high (0.04 μM and 0.07 μM) affinities. High and low affinity binding of human Fab and light chain of $V_κ1$-subgroup type to 2 distinct sites on single Ig binding domains of protein L have been reported previously.[63,64] Here a differential V_L:protein L stoichiometry was also observed, with the λ type V_L having a 1:1 binding stoichiometry, the $V_κ3$ V_Ls having a 3:1 binding stoichiometry in the majority of cases, and $V_κ1$ having a 7:1 binding stoichiometry. Previous SPR binding studies with 5 Ig-binding domains of a protein L showed that while all 5 domains bound to a human $V_κ$ light chain of $V_κ1$ subgroup, only 3 bound to a human $V_κ$ light chain of $V_κ3$ subgroup, supporting the higher observed stoichiometry for $V_κ1$ binders compared with $V_κ3$ binders and the 3:1 stoichiometry found for the $V_κ3$ binders. A binding stoichiometry of 7:1 in the case $V_κ1$ subgroup binders is plausible, given that our protein L consisted of 4 Ig-binding domains with each Ig-binding domain having up to 2 binding sites that can simultaneously engage with 2 sites on $V_κ1$ subgroup binders.[63,64,71] A higher affinity and stoichiometry (higher avidity) in the case of $V_κ1$ type antibodies should translate to their more sensitive detection by protein L. The low affinity and lack of avidity as a result of a 1:1 stoichiometry, as shown here for the $V_λ$ type HVLP389, may be the reason for the reported weak interactions between human Ig λ-light chains and protein L.[41,65,66] Thus, failing to detect a $V_λ$-protein L interaction should not be interpreted as the lack of protein L binding activity on the part of a $V_λ$ type antibody. It should, however, be mentioned that the stoichiometry values are estimates. If the surface is not fully active the theoretical R_{max} for 1:1 binding cannot be

attained, resulting in underestimation of the binding stoichiometry. Isothermal titration calorimetry may provide a more accurate means of determining the binding stoichiometries.

Consistent with being highly non-aggregating at concentrations as high as ≈450 μM, the V_Ls showed high reversibility of thermal unfolding at relatively high V_L concentrations. In this respect, and with respect to T_m, the V_Ls performed as well as our set of non-aggregating V_Hs. The observed lack of correlation between T_m and aggregation resistance, expressed in terms of TREs, is consistent with previous findings that showed that aggregation resistant V_Hs may not necessarily have high T_m or thermodynamic stability.[72] Consistent with this finding is the fact that the V_L with the highest T_m from among the eight V_Ls in this study (HVLP325) was also the only one that showed some degree of aggregation.

The V_Ls were different from V_Hs with respect to GI protease resistance patterns. That is, while V_Ls were more resistant to chymotrypsin, the V_Hs were more so to pepsin, with both V_Ls and V_Hs being comparable in terms of resistance to trypsin. The observed protease resistance data for only chymotrypsin could be explained in terms of the number of potential cleavage sites, i.e., V_Ls had a significantly lower number of potential chymotrypsin cleavage sites than V_Hs. Even when only the more protease accessible CDR sequences were considered in the calculation of theoretical number of cleavage sites, the obtained numbers did not fully explain the observed differences between protease resistance profiles of V_Ls and V_Hs (data not shown). Previously for V_HHs, increases in pepsin resistance were correlated with increases in T_ms, but this correlation cannot explain the better pepsin resistance of V_Hs here because both V_Hs and V_Ls had very similar T_ms.[49] As discussed previously, protease sensitivity is a function of a number of variables including the theoretical number of proteolytic sites, the location of proteolytic sites, and protein compactness and thermodynamic stability.[49,73,74]

In an effort to further improve the biophysical properties of V_Ls, we introduced a pair of cysteine residues at amino acid positions 48 and 64, hypothesizing that this would lead to the formation of a disulfide linkage in the sdAb core. Previously, it was shown that the substitution for a pair of cysteine at spatially equivalent positions in V_HHs and V_Hs led to the formation of disulfide linkages in all domains tested, with subsequent improvements in thermostability and protease resistance.[46,49-52] We too find here that all the V_Ls with the added Cys pair have the intended disulfide linkage, as well as improved thermostability (T_m) and protease resistance. We find that the increases in T_ms (ΔT_m) are relatively high (5.4–17.3 °C, median ΔT_m: 12.4 °C) compared with those obtained for a previously reported set of V_HHs with similar engineered disulfide linkages (ΔT_m: 4–12 °C, median ΔT_m: 7 °C).[49] This may, at least partly, be due to the fact that T_ms were obtained under different assay conditions and instrument settings. It cannot be excluded, however, that a non-canonical disulfide linkage may have been a better fit to the overall fold of V_Ls, leading to their overall higher ΔT_m gains.[49] This may also explain the differential T_m gains observed among the mutant V_Ls that were characterized under identical conditions. We also find that the thermostability gain due to the engineered disulfide linkage is more pronounced for the κ3 and λ1 members, compared with the κ1 members; however, general conclusions should await further experiments involving a statistically appropriate sample size.

In terms of protease resistance, the non-canonical disulfide linkage led to increases in pepsin resistance of V_Ls, without compromising their trypsin or chymotrypsin resistance. This is similar to the results obtained with a set of V_HHs with similar non-canonical disulfide linkages.[49] As with the V_HHs, positive correlations between pepsin resistance and T_m were also observed. The higher pepsin resistance of the mutant V_Ls may be due to the fact that they may have a more compact and thermodynamically stable structure—equating to higher resistance to acid-induced unfolding under pepsin digestion conditions (pH = 2; pepsin is more effective on denatured proteins)—compared with the wild-type V_Ls without the non-canonical disulfide linkage.[49] Higher T_ms of mutants, suggesting their higher thermodynamic stabilities, and the fact that V_HHs with similar engineered disulfide linkage became resistant to unfolding at pH 2 and 37 °C support this speculation.[49] Importantly, the introduction of the non-canonical disulfide linkage into V_Ls does not appear to compromise their aggregation resistance. This was shown to be the case for V_HHs and V_Hs with similar non-canonical disulfide linkages as well.[46,49] In the case of V_Hs, this led to improvements in the aggregation resistance of mutants compared with the wild-type counterparts without the non-canonical disulfide linkage.

The biophysical improvements gained through the introduction of the non-canonical disulfide linkage do come at the expense of expression yield as mutants demonstrated significantly lower expression yields than wild-type V_Ls in *E. coli*. This was also reported in the case of V_HHs, which like the V_Ls here, were expressed in *E. coli*.[49] Thus, the relatively lower expression yields of Cys mutant domains compared with wild-type ones may have to do with the limited capacity of *E. coli* in folding proteins with higher disulfide linkages such as the Cys mutant V_Ls in this study. This should be resolved by expressing the mutant V_Ls in eukaryotic microorganisms, e.g., yeast or mammalian cells, with the capacity to fold complex proteins such as those with multiple disulfide linkages.

The biophysical improvements also come at the expense of undesirable conformational changes for mutants, which were also reported in the case of V_HHs and V_Hs.[46,49] The observed differential protease resistance profiles between wild-type and corresponding mutant V_Ls, as well as changes to protein L binding for some of the mutants, support this conclusion. However, for the majority of V_Ls, the conformational changes, as determined by binding measurements of wild-type and Cys mutant V_Ls against protein L, are too subtle to be sensed by protein L, which binds to V_Ls in a conformation-dependent manner.[41] This is in sharp contrast to the results obtained with our Cys mutant V_Hs,[46] where structural changes as a result of the introduction of non-canonical disulfide linkages were more easily probed with protein A and led to up to 10-fold reductions in protein A binding of mutant V_Hs. Such discrepancy could be due to the fact that, while for V_Ls the protein L binding site is too far from the engineered disulfide linkage to be affected by it, for V_Hs the protein A binding site

is in the influencing range of the non-canonical disulfide linkage. This is clearly supported by our homology structure data of a V_L and a V_H with similar non-canonical disulfide linkages (*see* **Figure 7**). The conformational changes in V_L mutants were not reflected in SPR stoichiometry data either, as all wild-type/mutant pairs had the same stoichiometry of binding to protein L.

In conclusion, we demonstrated the suitability of V_L sdAbs as affinity reagents, in particular, as immunotherapeutics, and provided insights into the biophysical characteristics of V_Ls. We identified a diversity of non-aggregating V_L domains that could form the basis of therapeutics when incorporated as library scaffolds (e.g., into sdAb phage display libraries) as has already been demonstrated.[32] As, irrespective of the degree of the stability of the original library scaffold, loop randomization always leads to a proportion of the library consisting of unstable domains, a coupling of affinity selection to stability selection during the panning experiments to filter out unstable binders from the pool of binders is advisable.[53,55,72,75] Moreover, we presented a general strategy based on disulfide linkage engineering for stabilizing V_Ls in terms of thermostability and pepsin resistance. The disulfide linkage engineered V_Ls would be the preferred scaffolds for constructing V_L phage display libraries over versions without. Such libraries, especially if affinity selected under high temperature conditions, should yield non-aggregating immunotherapeutics that are also thermodynamically stable, like those V_H domains that were selected by panning a phage display library under the acidic conditions.[72] Due to the positive correlation between pepsin resistance and T_m, affinity selection under heat should yield binders which are also pepsin resistant, hence suitable as oral therapeutics for GI tract applications. The disulfide linkage engineering approach should thus be viewed as an efficacy engineering one for therapeutic V_Ls. The fact that the affinity reagents obtained from the aforementioned V_L libraries would have protein L binding properties offers biotechnological advantages similar to those offered by V_Hs that bind to B cell superantigen protein A.[48]

Beyond single domains, the disulfide linkage engineering approach can be applied to domains in the context of scFvs, Fabs, and IgGs. Previously, when a similar disulfide linkage engineering approach was applied to a V_H in the context of a Fab, it resulted in a significant increase in the thermostability of the Fab.[76] However, the introduction of the disulfide linkage results in conformational changes that may further lead to undesirable affinity and specificity compromises as has been shown in the case of V_HHs with similar disulfide linkage engineering.[49-51] This should not be a concern with domains that are selected from libraries already containing the non-canonical disulfide linkage.

Materials and Methods

Human V_L library construction and panning

A V_L phage display library in a multivalent display format and with plaque formation as the selectable marker was constructed in a similar fashion as a previously described V_H phage display library.[48] It was anticipated that, as in the case of the V_H phage display library, phages displaying non-aggregating domains (V_Ls in the present study) would form larger plaques on bacterial lawns than phages displaying aggregation prone domains, and, as a result, panning the library against super-antigen protein L for several cycles should eventually enrich the library for phage-displayed, aggregation-resistant V_Ls that bind protein L. Such V_Ls can subsequently be retrieved and expressed as soluble, autonomous domains. Briefly, cDNA was synthesized from human spleen mRNA as previously described.[48] The cDNA was used as a template for PCR to amplify V_L genes in 50 μL reaction volumes using six V_κ and 11 V_λ back primers[77] and four V_κ and two V_λ forward primers.[78] The back and forward primers were modified to have flanking ApaLI and NotI restriction sites, respectively, for subsequent cloning purposes. Forward primers were pooled together in ratios that reflected their degree of degeneracy. V_λ genes were subjected to PCR in 11 separate reactions using the pooled V_λ forward primers with 11 individual V_λ back primers. Similarly, V_κ genes were amplified in six separate reactions using the pooled V_κ forward primers with six individual V_κ back primers. The PCR products were gel-purified and digested with ApaLI and NotI restriction endonucleases, and the library was constructed as previously described.[48] PCR was performed on individual library colonies, and the amplified V_L genes were sequenced as described before.[79] Panning (against protein L; Pierce) and the germline assignment of V_Ls were performed as previously described.[48]

Cloning, expression, purification, SEC, and MALS analysis

Introduction of cysteine residues at Kabat positions 48 and 64[43] of V_Ls was performed using a splice overlap extension method.[46] V_L expression, purification, concentration determination, and SEC were performed as described for V_Hs.[47,55] Size-exclusion chromatograms were normalized as described.[46,47] The elution volume values obtained from chromatograms were used to calculate M_{app}s of V_Ls using the Log M *vs.* V_e standard curve described in **Figure S1**. UPLC-SEC-MALS was performed with a Waters BioAcquity system equipped with a Waters PDA detector (Waters). The column temperature was maintained at 30 °C with a CM-A column compartment. The samples (10–20 μg) were injected onto a Waters BEH125 SEC column (4.6 mm × 150 mm, 1.7 μm particles) at 0.4 mL/min with PBS (–Ca –Mg, Hyclone Thermo Scientific) as the solvent. MALS data was measured on a Wyatt HELEOS 8+ detector (Wyatt Technology Corporation) and weight average molecular masses (M_{MALS}s) were calculated using a protein concentration determined using the A_{280} from the PDA detector with extinction coefficients calculated from the amino acid sequences. Experiments were performed in duplicates. MALS data processing was performed with ASTRA 6.1 software (Wyatt Technology Corporation).

Disulfide linkage determination

Disulfide linkage determination for Cys mutant V_Ls was performed as described elsewhere.[46,49] Briefly, tryptic fragments for subsequent MS analysis were prepared as described.[47] Purified V_Ls at ~15 pmol/μL in 50% (v/v) acetonitrile + 0.1% (v/v) formic acid were infused at 1 μL/min for electrospray ionization (ESI) mass spectrometric mass measurements of the V_Ls using a Q-TOF 2™ mass spectrometer (Waters). The mass spectra of the V_Ls were de-convoluted using the MaxEnt 1 program in

the MassLynx software package (Waters). Aliquots of V_L proteolytic digests were re-suspended in 0.1% (v/v) formic acid (aq) and subsequently analyzed by nano-flow reversed-phase HPLC MS (nanoRPLC-ESI-MS) with data-dependent analysis (DDA) using CID on a nanoAcquity UPLC system coupled to a Q-TOF Ultima™ hybrid quadrupole/TOF mass spectrometer (Waters). The peptides were first loaded onto a 180 μm I.D. × 20 mm 5 μm symmetry®C18 trap (Waters) and then eluted into a 100 μm I.D. × 10 cm 1.7 μm BEH130C18 column (Waters) using a linear gradient from 0% to 36% solvent B (acetonitrile + 0.1% formic acid) over 36 min followed by 36–90% solvent B for 2 min. Solvent A was 0.1% formic acid in water. The peptide MS^2 spectra were compared with mutant V_L protein sequences using the Mascot™ database searching algorithm (Matrix Science). The MS^2 spectra of the disulfide-linked peptides were de-convoluted using the MaxEnt 3 program (Waters) for de novo sequencing to confirm and determine the exact disulfide linkage positions. NanoRPLC-ESI-MS analyses with DDA using a combination of ETD and CID were performed on an LTQXL mass spectrometer fitted with an ETD source (Thermo Fisher Scientific) and coupled to a nanoAcquity UPLC system (Waters) using the LC conditions described above. Briefly, for the DDA experiments, the most abundant peptide ion from the survey scan was used for the automatic acquisition of ETD-MS^2 spectra using 30% normalized collision energy followed by the acquisition of ETD-CID-MS^3 spectra of the most abundant charge-reduced ions produced by ETD.

SPR binding studies

V_Ls were subjected to Superdex 75™ (GE Healthcare) SEC in HBS-EP buffer (10 mM HEPES, pH 7.4, 150 mM NaCl, 3 mM EDTA and 0.005% P20 surfactant) at 0.5 mL/min prior to BIACORE analysis and purified monomer peaks were collected even in the absence of any evidence of aggregated material. Binding kinetics for the interaction of V_Ls to protein L were determined by SPR using a BIACORE 3000 biosensor system (GE Healthcare). For wild-type V_Ls, ~600 resonance units (RUs) of protein L or 800 RUs of a Fab reference were immobilized onto research grade CM5 sensorchips (GE Healthcare). For mutant V_Ls, ~650 RUs of protein L (for HVLP324S, HVLP325S, and HVLP342S) or 400 RUs of protein L (for HVLP335S, HVLP351S, HVLP389S, and HVLP3103S) or 400 RUs of ovalbumin (Sigma-Aldrich) as a reference protein were immobilized. For HVLP324S and HVLP342S, ~1,700 RUs of protein L or 2,600 RUs of a ovalbumin reference were immobilized onto research grade CM5 sensorchips to determine binding data for the low affinity binding sites on protein L. Immobilization was performed at protein concentrations of 20 or 50 μg/mL in 10 mM acetate buffer, pH 4.5, using an amine coupling kit supplied by the manufacturer (GE Healthcare). All measurements were performed at 25 °C in HBS-EP buffer at 40 or 50 μL/min. The surfaces were regenerated through washing with the running buffer. Data were evaluated using BIAevaluation 4.1 software (GE Healthcare). The stoichiometry of binding (V_L:protein L) was estimated by comparing the observed R_{max}s and theoretical R_{max}s for 1:1 binding.

SPR analysis for the binding of V_Ls, a control llama V_HH monomer (A4.2), and a control V_H homodimer to a Ni^{2+}-NTA sensorchip was performed as described previously.[46] All V_L/V_H/V_HH domains had His_6 tags at their C-termini and the protein preparations lacked contaminating species without the His_6 tag as determined by Western blot and SDS-PAGE analyses. The V_H homodimer is formed by the non-covalent association of two V_H monomer units, and, as a result, has two C-terminal His_6 tags. SPR experiments were performed with protein fractions corresponding to the dimeric peak in the case of the V_H dimer control and monomeric peaks for the remaining V_L/V_HH domains. RUs from duplicate data sets were averaged and then normalized to obtain %RU. The SPR binding of antibody domains to an activated NTA sensorchip was determined at 25 °C using a BIACORE 3000. In each cycle, $NiCl_2$ was injected, followed by an injection of V_L/V_H/V_HH. Sensorgrams were run in duplicates. The NTA chip was regenerated with EDTA before the next cycle. Dissociation rate constants (k_{off}s) were obtained over 60 s periods between 315–375 s and 780–840 s and data were analyzed with BIAevaluation 4.1 software.

Protease digestion experiments

Digestion experiments were performed in a total volume of 30 μL with 6 μg of V_L in phosphate-buffered saline (137 mM NaCl, 2.7 mM KCl, 4.3 mM Na_2HPO_4, 1.47 mM KH_2PO_4, pH 7.4) at 37 °C for 1 h with an enzyme to V_L ratio of 1:200, 1:40, 1:20, and 1:10 (trypsin/chymotrypsin), corresponding to 1 μg/mL, 5 μg/mL, 10 μg/mL, and 20 μg/mL protease concentrations, respectively, or 1:200, 1:20, 1:10, and 1:4 (pepsin), which corresponds to 1 μg/mL, 10 μg/mL, 20 μg/mL, and 50 μg/mL protease concentrations, respectively. Tryptic and chymotryptic digestion experiments were performed using sequencing grade enzymes (Roche Diagnostics) according to the manufacturer's instructions. Peptic digestion experiments were performed at pH 2.0 using pepsin from Sigma-Aldrich. In control experiments, enzymes were replaced with equal volumes of reaction buffers. Reactions were stopped by adding an equal volume of SDS-PAGE sample buffer containing 0.2 M dithiothreitol and boiling mixtures at 95 °C for 5 min. The samples were then subjected to SDS-PAGE analysis and the percentages of intact sdAbs after protease digestions were determined by spot density analysis as described.[49] For V_Hs, digestion experiments were performed as described for V_Ls with an enzyme to V_H ratio of 1:20.

TRE experiments

TREs were determined by SPR as previously described.[48] Briefly, V_Ls or V_Hs were incubated at 85 °C for 20 min at concentrations of 4 or 20 μM, slowly cooled to room temperature for 30 min, centrifuged at 16,000 X *g* for 5 min at 22 °C, and the supernatants, termed "refolded," were kept for subsequent SPR analysis. Following this, binding analysis against protein L and protein A for V_Ls and V_Hs, respectively, was performed. Native and refolded domains were analyzed under identical conditions. For V_Ls at 4 μM, 600 RUs of protein L and 700 RUs of a Fab reference were immobilized at 25 or 50 μg/mL in 10 mM acetate buffer, pH 4.5. For V_Hs at 4 μM, 600 RUs of protein A (Sigma-Aldrich) or ovalbumin reference were immobilized at 50 μg/

mL in 10 mM acetate buffer, pH 4.5. For V_Ls at 20 μM, 2,100 RUs of protein L and 1,200 RUs of ovalbumin reference were immobilized at 100 μg/mL in acetate buffer, pH 4.0, and 50 μg/mL in 10 mM acetate buffer, pH 4.5, respectively. For V_Hs at 20 μM, 650–1,100 RUs of protein A and 600–1,200 RUs of ovalbumin were immobilized at 50 μg/mL in 10 mM acetate buffer, pH 4.5. In all instances, the analyses were performed at 25 °C in HBS-EP buffer at 40 μL/min. The surfaces were washed thoroughly with the running buffer for regeneration. Data were analyzed with BIAevaluation 4.1 software and K_Ds were analyzed with 1:1 binding models. Refolding efficiencies were expressed in terms of the ratio of K_D (refolded)/K_D (native).[48]

T_m measurements

Circular dichroism spectra and T_ms of V_Ls and V_Hs were obtained as described previously[47,49] using a Jasco J-815 spectropolarimeter (Jasco) equipped with a Peltier thermoelectric type temperature control system. The circular dichroism spectra were recorded over a temperature range of 30 °C to 96 °C in 100 mM sodium phosphate buffer, pH 7.4, and with a protein concentration of 50 μg/mL. Ellipticity changes at 203 nm for HVLP325 and HVLP389, at 218 nm for HVLP324, HVLP335, HVLP342, HVLP351, HVLP364, and HVLP3103, at 210 nm for Cys mutant V_Ls, at 205 nm for HVHP421, HVHP428, and HVHP429, at 200 nm for HVHP413, HVHP419, and HVHP420, and at 202 nm for HVHP44 and HVHP414 were used for constructing thermal unfolding curves and subsequent calculations of T_ms. At these wavelengths, wide differences in ellipticity values between the folded (at 30 °C) and fully denatured (at 90 °C) domains allowed reliable determination of T_ms (**Fig. S6**).

Disclosure of Potential Conflicts of Interest

No potential conflicts of interest were disclosed.

Acknowledgments

We thank Sonia Leclerc for DNA sequencing.

Supplemental Materials

Supplemental materials can be found at www.landesbioscience.com/journals/mabs/article/26844

References

1. Fox JL. Anthrax drug first antibacterial mAb to win approval. Nat Biotechnol 2013; 31:8; PMID:23302914; http://dx.doi.org/10.1038/nbt0113-8
2. Nelson AL. Antibody fragments: hope and hype. MAbs 2010; 2:77-83; PMID:20093855; http://dx.doi.org/10.4161/mabs.2.1.10786
3. Nelson AL, Reichert JM. Development trends for therapeutic antibody fragments. Nat Biotechnol 2009; 27:331-7; PMID:19352366; http://dx.doi.org/10.1038/nbt0409-331
4. Holliger P, Hudson PJ. Engineered antibody fragments and the rise of single domains. Nat Biotechnol 2005; 23:1126-36; PMID:16151406; http://dx.doi.org/10.1038/nbt1142
5. Holt LJ, Herring C, Jespers LS, Woolven BP, Tomlinson IM. Domain antibodies: proteins for therapy. Trends Biotechnol 2003; 21:484-90; PMID:14573361; http://dx.doi.org/10.1016/j.tibtech.2003.08.007
6. Ma X, Barthelemy PA, Rouge L, Wiesmann C, Sidhu SS. Design of synthetic autonomous V_H domain libraries and structural analysis of a V_H domain bound to vascular endothelial growth factor. J Mol Biol 2013; 425:2247-59; PMID:23507309; http://dx.doi.org/10.1016/j.jmb.2013.03.020
7. Matz J, Kessler P, Bouchet J, Combes O, Ramos OH, Barin F, Baty D, Martin L, Benichou S, Chames P. Straightforward selection of broadly neutralizing single-domain antibodies targeting the conserved CD4 and coreceptor binding sites of HIV-1 gp120. J Virol 2013; 87:1137-49; PMID:23152508; http://dx.doi.org/10.1128/JVI.00461-12
8. Mukherjee J, Tremblay JM, Leysath CE, Ofori K, Baldwin K, Feng X, Bedenice D, Webb RP, Wright PM, Smith LA, et al. A novel strategy for development of recombinant antitoxin therapeutics tested in a mouse botulism model. PLoS One 2012; 7:e29941; PMID:22238680; http://dx.doi.org/10.1371/journal.pone.0029941
9. Jamnani FR, Rahbarizadeh F, Shokrgozar MA, Ahmadvand D, Mahboudi F, Sharifzadeh Z. Targeting high affinity and epitope-distinct oligoclonal nanobodies to HER2 over-expressing tumor cells. Exp Cell Res 2012; 318:1112-24; PMID:22440788; http://dx.doi.org/10.1016/j.yexcr.2012.03.004
10. Wei G, Meng W, Guo H, Pan W, Liu J, Peng T, Chen L, Chen CY. Potent neutralization of influenza A virus by a single-domain antibody blocking M2 ion channel protein. PLoS One 2011; 6:e28309; PMID:22164266; http://dx.doi.org/10.1371/journal.pone.0028309
11. Trilling AK, de Ronde H, Noteboom L, van Houwelingen A, Roelse M, Srivastava SK, Haasnoot W, Jongsma MA, Kolk A, Zuilhof H, et al. A broad set of different llama antibodies specific for a 16 kDa heat shock protein of *Mycobacterium tuberculosis*. PLoS One 2011; 6:e26754; PMID:22046343; http://dx.doi.org/10.1371/journal.pone.0026754
12. Skottrup PD, Leonard P, Kaczmarek JZ, Veillard F, Enghild JJ, O'Kennedy R, Sroka A, Clausen RP, Potempa J, Riise E. Diagnostic evaluation of a nanobody with picomolar affinity toward the protease RgpB from *Porphyromonas gingivalis*. Anal Biochem 2011; 415:158-67; PMID:21569755; http://dx.doi.org/10.1016/j.ab.2011.04.015
13. Goldman ER, Anderson GP, Zabetakis D, Walper S, Liu JL, Bernstein R, Calm A, Carney JP, O'Brien TW, Walker JL, et al. Llama-derived single domain antibodies specific for *Abrus* agglutinin. Toxins (Basel) 2011; 3:1405-19; PMID:22174977; http://dx.doi.org/10.3390/toxins3111405
14. Emmerson CD, van der Vlist EJ, Braam MR, Vanlandschoot P, Merchiers P, de Haard HJW, Verrips CT, van Bergen en Henegouwen PM, Dolk E. Enhancement of polymeric immunoglobulin receptor transcytosis by biparatopic VHH. PLoS One 2011; 6:e26299; PMID:22022593; http://dx.doi.org/10.1371/journal.pone.0026299
15. Hmila I, Saerens D, Ben Abderrazek R, Vincke C, Abidi N, Benlasfar Z, Govaert J, El Ayeb M, Bouhaouala-Zahar B, Muyldermans S. A bispecific nanobody to provide full protection against lethal scorpion envenoming. FASEB J 2010; 24:3479-89; PMID:20410443; http://dx.doi.org/10.1096/fj.09-148213
16. Monegal A, Ami D, Martinelli C, Huang H, Aliprandi M, Capasso P, Francavilla C, Ossolengo G, de Marco A. Immunological applications of single-domain llama recombinant antibodies isolated from a naïve library. Protein Eng Des Sel 2009; 22:273-80; PMID:19196718; http://dx.doi.org/10.1093/protein/gzp002
17. Li S, Zheng W, Kuolee R, Hirama T, Henry M, Makvandi-Nejad S, Fjällman T, Chen W, Zhang J. Pentabody-mediated antigen delivery induces antigen-specific mucosal immune response. Mol Immunol 2009; 46:1718-26; PMID:19269688; http://dx.doi.org/10.1016/j.molimm.2009.02.007
18. Deckers N, Saerens D, Kanobana K, Conrath K, Victor B, Wernery U, Vercruysse J, Muyldermans S, Dorny P. Nanobodies, a promising tool for species-specific diagnosis of *Taenia solium* cysticercosis. Int J Parasitol 2009; 39:625-33; PMID:19041315; http://dx.doi.org/10.1016/j.ijpara.2008.10.012
19. Abderrazek RB, Hmila I, Vincke C, Benlasfar Z, Pellis M, Dabbek H, Saerens D, El Ayeb M, Muyldermans S, Bouhaouala-Zahar B. Identification of potent nanobodies to neutralize the most poisonous polypeptide from scorpion venom. Biochem J 2009; 424:263-72; PMID:19732033; http://dx.doi.org/10.1042/BJ20090697
20. Koide A, Tereshko V, Uysal S, Margalef K, Kossiakoff AA, Koide S. Exploring the capacity of minimalist protein interfaces: interface energetics and affinity maturation to picomolar K_D of a single-domain antibody with a flat paratope. J Mol Biol 2007; 373:941-53; PMID:17888451; http://dx.doi.org/10.1016/j.jmb.2007.08.027
21. Kopsidas G, Roberts AS, Coia G, Streltsov VA, Nuttall SD. *In vitro* improvement of a shark IgNAR antibody by Qß replicase mutation and ribosome display mimics *in vivo* affinity maturation. Immunol Lett 2006; 107:163-8; PMID:17069896; http://dx.doi.org/10.1016/j.imlet.2006.09.004
22. Shen J, Vil MD, Jimenez X, Iacolina M, Zhang H, Zhu Z. Single variable domain-IgG fusion. A novel recombinant approach to Fc domain-containing bispecific antibodies. J Biol Chem 2006; 281:10706-14; PMID:16481314; http://dx.doi.org/10.1074/jbc.M513415200
23. Colby DW, Chu Y, Cassady JP, Duennwald M, Zazulak H, Webster JM, Messer A, Lindquist S, Ingram VM, Wittrup KD. Potent inhibition of huntingtin aggregation and cytotoxicity by a disulfide bond-free single-domain intracellular antibody. Proc Natl Acad Sci U S A 2004; 101:17616-21; PMID:15598740; http://dx.doi.org/10.1073/pnas.0408134101

24. Cortez-Retamozo V, Backmann N, Senter PD, Wernery U, De Baetselier P, Muyldermans S, Revets H. Efficient cancer therapy with a nanobody-based conjugate. Cancer Res 2004; 64:2853-7; PMID:15087403; http://dx.doi.org/10.1158/0008-5472.CAN-03-3935
25. Nuttall SD, Humberstone KS, Krishnan UV, Carmichael JA, Doughty L, Hattarki M, Coley AM, Casey JL, Anders RF, Foley M, et al. Selection and affinity maturation of IgNAR variable domains targeting *Plasmodium falciparum* AMA1. Proteins 2004; 55:187-97; PMID:14997552; http://dx.doi.org/10.1002/prot.20005
26. Saerens D, Kinne J, Bosmans E, Wernery U, Muyldermans S, Conrath K. Single domain antibodies derived from dromedary lymph node and peripheral blood lymphocytes sensing conformational variants of prostate-specific antigen. J Biol Chem 2004; 279:51965-72; PMID:15459193; http://dx.doi.org/10.1074/jbc.M409292200
27. Nuttall SD, Krishnan UV, Doughty L, Pearson K, Ryan MT, Hoogenraad NJ, Hattarki M, Carmichael JA, Irving RA, Hudson PJ. Isolation and characterization of an IgNAR variable domain specific for the human mitochondrial translocase receptor Tom70. Eur J Biochem 2003; 270:3543-54; PMID:12919318; http://dx.doi.org/10.1046/j.1432-1033.2003.03737.x
28. Tanaka T, Lobato MN, Rabbitts TH. Single domain intracellular antibodies: a minimal fragment for direct *in vivo* selection of antigen-specific intrabodies. J Mol Biol 2003; 331:1109-20; PMID:12927545; http://dx.doi.org/10.1016/S0022-2836(03)00836-2
29. Davies J, Riechmann L. Affinity improvement of single antibody VH domains: residues in all three hypervariable regions affect antigen binding. Immunotechnology 1996; 2:169-79; PMID:9373310; http://dx.doi.org/10.1016/S1380-2933(96)00045-0
30. Arbabi-Ghahroudi M, Tanha J, MacKenzie R. Prokaryotic expression of antibodies. Cancer Metastasis Rev 2005; 24:501-19; PMID:16408159; http://dx.doi.org/10.1007/s10555-005-6193-1
31. Muyldermans S. Single domain camel antibodies: current status. J Biotechnol 2001; 74:277-302; PMID:11526908
32. Hussack G, Keklikian A, Alsughayyir J, Hanifi-Moghaddam P, Arbabi-Ghahroudi M, van Faassen H, Hou ST, Sad S, MacKenzie R, Tanha J. A V_L single-domain antibody library shows a high-propensity to yield non-aggregating binders. Protein Eng Des Sel 2012; 25:313-8; PMID:22490957; http://dx.doi.org/10.1093/protein/gzs014
33. Ewert S, Huber T, Honegger A, Plückthun A. Biophysical properties of human antibody variable domains. J Mol Biol 2003; 325:531-53; PMID:12498801; http://dx.doi.org/10.1016/S0022-2836(02)01237-8
34. Dubnovitsky AP, Kravchuk ZI, Chumanevich AA, Cozzi A, Arosio P, Martsev SP. Expression, refolding, and ferritin-binding activity of the isolated VL-domain of monoclonal antibody F11. Biochemistry (Mosc) 2000; 65:1011-8; PMID:11042491
35. Tomlinson IM, Cox JP, Gherardi E, Lesk AM, Chothia C. The structural repertoire of the human Vκ domain. EMBO J 1995; 14:4628-38; PMID:7556106
36. Lefranc MP. Nomenclature of the human immunoglobulin lambda (IGL) genes. Exp Clin Immunogenet 2001; 18:242-54; PMID:11872955; http://dx.doi.org/10.1159/000049203
37. Lefranc MP. Nomenclature of the human immunoglobulin kappa (IGK) genes. Exp Clin Immunogenet 2001; 18:161-74; PMID:11549845; http://dx.doi.org/10.1159/000049195
38. Knappik A, Ge L, Honegger A, Pack P, Fischer M, Wellnhofer G, Hoess A, Wölle J, Plückthun A, Virnekäs B. Fully synthetic human combinatorial antibody libraries (HuCAL) based on modular consensus frameworks and CDRs randomized with trinucleotides. J Mol Biol 2000; 296:57-86; PMID:10656818; http://dx.doi.org/10.1006/jmbi.1999.3444
39. Viau M, Longo NS, Lipsky PE, Björck L, Zouali M. Specific *in vivo* deletion of B-cell subpopulations expressing human immunoglobulins by the B-cell superantigen protein L. Infect Immun 2004; 72:3515-23; PMID:15155659; http://dx.doi.org/10.1128/IAI.72.6.3515-3523.2004
40. Åkerström B, Nilson BH, Hoogenboom HR, Björck L. On the interaction between single chain Fv antibodies and bacterial immunoglobulin-binding proteins. J Immunol Methods 1994; 177:151-63; PMID:7822821; http://dx.doi.org/10.1016/0022-1759(94)90152-X
41. Nilson BH, Solomon A, Björck L, Åkerström B. Protein L from *Peptostreptococcus magnus* binds to the κ light chain variable domain. J Biol Chem 1992; 267:2234-9; PMID:1733930
42. Bork P, Holm L, Sander C. The immunoglobulin fold. Structural classification, sequence patterns and common core. J Mol Biol 1994; 242:309-20; PMID:7932691; http://dx.doi.org/10.1016/S0022-2836(84)71582-8
43. Kabat EA, Wu TT, Perry HM, Gottesman KS, Foeller C. Sequences of Proteins of Immunological Interest, 5th ed., National Institutes of Health Publication 91-3242, National Institutes of Health, Bethesda, MD 1991.
44. Lesk AM, Chothia C. Evolution of proteins formed by β-sheets. II. The core of the immunoglobulin domains. J Mol Biol 1982; 160:325-42; PMID:7175935; http://dx.doi.org/10.1016/0022-2836(82)90179-6
45. Amzel LM, Poljak RJ. Three-dimensional structure of immunoglobulins. Annu Rev Biochem 1979; 48:961-97; PMID:89832; http://dx.doi.org/10.1146/annurev.bi.48.070179.004525
46. Kim DY, Kandalaft H, Ding W, Ryan S, van Faassen H, Hirama T, Foote SJ, MacKenzie R, Tanha J. Disulfide linkage engineering for improving biophysical properties of human V_H domains. Protein Eng Des Sel 2012; 25:581-9; PMID:22942392; http://dx.doi.org/10.1093/protein/gzs055
47. Kim DY, Ding W, Tanha J. Solubility and stability engineering of human V_H domains. Methods Mol Biol 2012; 911:355-72; PMID:22886262
48. To R, Hirama T, Arbabi-Ghahroudi M, MacKenzie R, Wang P, Xu P, Ni F, Tanha J. Isolation of monomeric human V_Hs by a phage selection. J Biol Chem 2005; 280:41395-403; PMID:16221664; http://dx.doi.org/10.1074/jbc.M509900200
49. Hussack G, Hirama T, Ding W, Mackenzie R, Tanha J. Engineered single-domain antibodies with high protease resistance and thermal stability. PLoS One 2011; 6:e28218; PMID:22140551; http://dx.doi.org/10.1371/journal.pone.0028218
50. Saerens D, Conrath K, Govaert J, Muyldermans S. Disulfide bond introduction for general stabilization of immunoglobulin heavy-chain variable domains. J Mol Biol 2008; 377:478-88; PMID:18262543; http://dx.doi.org/10.1016/j.jmb.2008.01.022
51. Chan PH, Pardon E, Menzer L, De Genst E, Kumita JR, Christodoulou J, Saerens D, Brans A, Bouillenne F, Archer DB, et al. Engineering a camelid antibody fragment that binds to the active site of human lysozyme and inhibits its conversion into amyloid fibrils. Biochemistry 2008; 47:11041-54; PMID:18816062; http://dx.doi.org/10.1021/bi8005797
52. Hagihara Y, Mine S, Uegaki K. Stabilization of an immunoglobulin fold domain by an engineered disulfide bond at the buried hydrophobic region. J Biol Chem 2007; 282:36489-95; PMID:17932041; http://dx.doi.org/10.1074/jbc.M707078200
53. Jespers L, Schon O, Famm K, Winter G. Aggregation-resistant domain antibodies selected on phage by heat denaturation. Nat Biotechnol 2004; 22:1161-5; PMID:15300256; http://dx.doi.org/10.1038/nbt1000
54. Arbabi-Ghahroudi M, Mackenzie R, Tanha J. Site-directed mutagenesis for improving biophysical properties of V_H domains. Methods Mol Biol 2010; 634:309-30; PMID:20676993; http://dx.doi.org/10.1007/978-1-60761-652-8_22
55. Arbabi-Ghahroudi M, To R, Gaudette N, Hirama T, Ding W, MacKenzie R, Tanha J. Aggregation-resistant V_Hs selected by in vitro evolution tend to have disulfide-bonded loops and acidic isoelectric points. Protein Eng Des Sel 2009; 22:59-66; PMID:19033278; http://dx.doi.org/10.1093/protein/gzn071
56. Wu SL, Jiang H, Lu Q, Dai S, Hancock WS, Karger BL. Mass spectrometric determination of disulfide linkages in recombinant therapeutic proteins using online LC-MS with electron-transfer dissociation. Anal Chem 2009; 81:112-22; PMID:19117448; http://dx.doi.org/10.1021/ac801560k
57. Schiefner A, Chatwell L, Körner J, Neumaier I, Colby DW, Volkmer R, Wittrup KD, Skerra A. A disulfide-free single-domain V_L intrabody with blocking activity towards huntingtin reveals a novel mode of epitope recognition. J Mol Biol 2011; 414:337-55; PMID:21968397; http://dx.doi.org/10.1016/j.jmb.2011.09.034
58. Lee WR, Jang JY, Kim JS, Kwon MH, Kim YS. Gene silencing by cell-penetrating, sequence-selective and nucleic-acid hydrolyzing antibodies. Nucleic Acids Res 2010; 38:1596-609; PMID:20007602; http://dx.doi.org/10.1093/nar/gkp1145
59. Paz K, Brennan LA, Iacolina M, Doody J, Hadari YR, Zhu Z. Human single-domain neutralizing intrabodies directed against Etk kinase: a novel approach to impair cellular transformation. Mol Cancer Ther 2005; 4:1801-9; PMID:16276002; http://dx.doi.org/10.1158/1535-7163.MCT-05-0174
60. Colby DW, Garg P, Holden T, Chao G, Webster JM, Messer A, Ingram VM, Wittrup KD. Development of a human light chain variable domain (V_L) intracellular antibody specific for the amino terminus of huntingtin via yeast surface display. J Mol Biol 2004; 342:901-12; PMID:15342245; http://dx.doi.org/10.1016/j.jmb.2004.07.054
61. van den Beucken T, van Neer N, Sablon E, Desmet J, Celis L, Hoogenboom HR, Hufton SE. Building novel binding ligands to B7.1 and B7.2 based on human antibody single variable light chain domains. J Mol Biol 2001; 310:591-601; PMID:11439026; http://dx.doi.org/10.1006/jmbi.2001.4703
62. Enever C, Tomlinson IM, Lund J, Levens M, Holliger P. Engineering high affinity superantigens by phage display. J Mol Biol 2005; 347:107-20; PMID:15733921; http://dx.doi.org/10.1016/j.jmb.2005.01.020
63. Housden NG, Harrison S, Housden HR, Thomas KA, Beckingham JA, Roberts SE, Bottomley SP, Graille M, Stura E, Gore MG. Observation and characterization of the interaction between a single immunoglobulin binding domain of protein L and two equivalents of human κ light chains. J Biol Chem 2004; 279:9370-8; PMID:14668335; http://dx.doi.org/10.1074/jbc.M312938200
64. Graille M, Stura EA, Housden NG, Beckingham JA, Bottomley SP, Beale D, Taussig MJ, Sutton BJ, Gore MG, Charbonnier JB. Complex between *Peptostreptococcus magnus* protein L and a human antibody reveals structural convergence in the interaction modes of Fab binding proteins. Structure 2001; 9:679-87; PMID:11587642; http://dx.doi.org/10.1016/S0969-2126(01)00630-X

65. Åkerström B, Björck L. Protein L: an immunoglobulin light chain-binding bacterial protein. Characterization of binding and physicochemical properties. J Biol Chem 1989; 264:19740-6; PMID:2479638
66. Björck L. Protein L. A novel bacterial cell wall protein with affinity for Ig L chains. J Immunol 1988; 140:1194-7; PMID:3125250
67. Stevens FJ, Westholm FA, Solomon A, Schiffer M. Self-association of human immunoglobulin κI light chains: role of the third hypervariable region. Proc Natl Acad Sci U S A 1980; 77:1144-8; PMID:6767243; http://dx.doi.org/10.1073/pnas.77.2.1144
68. Dudgeon K, Rouet R, Kokmeijer I, Schofield P, Stolp J, Langley D, Stock D, Christ D. General strategy for the generation of human antibody variable domains with increased aggregation resistance. Proc Natl Acad Sci U S A 2012; 109:10879-84; PMID:22745168; http://dx.doi.org/10.1073/pnas.1202866109
69. Gorlani A, Hulsik DL, Adams H, Vriend G, Hermans P, Verrips T. Antibody engineering reveals the important role of J segments in the production efficiency of llama single-domain antibodies in *Saccharomyces cerevisiae*. Protein Eng Des Sel 2012; 25:39-46; PMID:22143875; http://dx.doi.org/10.1093/protein/gzr057
70. Tanha J, Nguyen TD, Ng A, Ryan S, Ni F, Mackenzie R. Improving solubility and refolding efficiency of human V_Hs by a novel mutational approach. Protein Eng Des Sel 2006; 19:503-9; PMID:16971398; http://dx.doi.org/10.1093/protein/gzl037
71. Svensson HG, Wedemeyer WJ, Ekstrom JL, Callender DR, Kortemme T, Kim DE, Sjöbring U, Baker D. Contributions of amino acid side chains to the kinetics and thermodynamics of the bivalent binding of protein L to Ig κ light chain. Biochemistry 2004; 43:2445-57; PMID:14992582; http://dx.doi.org/10.1021/bi034873s
72. Famm K, Hansen L, Christ D, Winter G. Thermodynamically stable aggregation-resistant antibody domains through directed evolution. J Mol Biol 2008; 376:926-31; PMID:18199455; http://dx.doi.org/10.1016/j.jmb.2007.10.075
73. Hubbard SJ, Beynon RJ, Thornton JM. Assessment of conformational parameters as predictors of limited proteolytic sites in native protein structures. Protein Eng 1998; 11:349-59; PMID:9681867; http://dx.doi.org/10.1093/protein/11.5.349
74. Frenken LG, Egmond MR, Batenburg AM, Verrips CT. P*seudomonas glumae lipase*: increased proteolytic stability by protein engineering. Protein Eng 1993; 6:637-42; PMID:8234234; http://dx.doi.org/10.1093/protein/6.6.637
75. Christ D, Famm K, Winter G. Repertoires of aggregation-resistant human antibody domains. Protein Eng Des Sel 2007; 20:413-6; PMID:17720749; http://dx.doi.org/10.1093/protein/gzm037
76. McConnell AD, Spasojevich V, Macomber JL, Krapf IP, Chen A, Sheffer JC, Berkebile A, Horlick RA, Neben S, King DJ, et al. An integrated approach to extreme thermostabilization and affinity maturation of an antibody. Protein Eng Des Sel 2013; 26:151-64; PMID:23173178; http://dx.doi.org/10.1093/protein/gzs090
77. de Haard HJ, van Neer N, Reurs A, Hufton SE, Roovers RC, Henderikx P, de Bruïne AP, Arends JW, Hoogenboom HR. A large non-immunized human Fab fragment phage library that permits rapid isolation and kinetic analysis of high affinity antibodies. J Biol Chem 1999; 274:18218-30; PMID:10373423; http://dx.doi.org/10.1074/jbc.274.26.18218
78. Sblattero D, Bradbury A. A definitive set of oligonucleotide primers for amplifying human V regions. Immunotechnology 1998; 3:271-8; PMID:9530560; http://dx.doi.org/10.1016/S1380-2933(97)10004-5
79. Tanha J, Muruganandam A, Stanimirovic D. Phage display technology for identifying specific antigens on brain endothelial cells. Methods Mol Med 2003; 89:435-49; PMID:12958438
80. Dombkowski AA. Disulfide by Design™: a computational method for the rational design of disulfide bonds in proteins. Bioinformatics 2003; 19:1852-3; PMID:14512360; http://dx.doi.org/10.1093/bioinformatics/btg231
81. Baral TN, Chao SY, Li S, Tanha J, Arbabi-Ghahroudi M, Zhang J, Wang S. Crystal structure of a human single domain antibody dimer formed through V_H-V_H non-covalent interactions. PLoS One 2012; 7:e30149; PMID:22253912; http://dx.doi.org/10.1371/journal.pone.0030149
82. Graille M, Stura EA, Corper AL, Sutton BJ, Taussig MJ, Charbonnier JB, Silverman GJ. Crystal structure of a *Staphylococcus aureus* protein A domain complexed with the Fab fragment of a human IgM antibody: structural basis for recognition of B-cell receptors and superantigen activity. Proc Natl Acad Sci U S A 2000; 97:5399-404; PMID:10805799; http://dx.doi.org/10.1073/pnas.97.10.5399